

# Identification of Multivesicular Bodies as Prevacuolar Compartments in *Nicotiana tabacum* BY-2 Cells <sup>W</sup>

Yu Chung Tse,<sup>a,b</sup> Beixin Mo,<sup>a</sup> Stefan Hillmer,<sup>c</sup> Min Zhao,<sup>a</sup> Sze Wan Lo,<sup>a,b</sup> David G. Robinson,<sup>c</sup> and Liwen Jiang<sup>a,b,1</sup>

<sup>a</sup>Department of Biology, Chinese University of Hong Kong, Shatin, New Territories, Hong Kong, China

<sup>b</sup>Molecular Biotechnology Program, Chinese University of Hong Kong, Shatin, New Territories, Hong Kong, China

<sup>c</sup>Department of Cell Biology, Heidelberg Institute for Plant Sciences, University of Heidelberg, D-69120 Heidelberg, Germany

Little is known about the dynamics and molecular components of plant prevacuolar compartments (PVCs). We have demonstrated recently that vacuolar sorting receptor (VSR) proteins are concentrated on PVCs. In this study, we generated transgenic *Nicotiana tabacum* (tobacco) BY-2 cell lines expressing two yellow fluorescent protein (YFP)-fusion reporters that mark PVC and Golgi organelles. Both transgenic cell lines exhibited typical punctate YFP signals corresponding to distinct PVC and Golgi organelles because the PVC reporter colocalized with VSR proteins, whereas the Golgi marker colocalized with mannosidase I in confocal immunofluorescence. Brefeldin A induced the YFP-labeled Golgi stacks but not the YFP-marked PVCs to form typical enlarged structures. By contrast, wortmannin caused YFP-labeled PVCs but not YFP-labeled Golgi stacks to vacuolate. VSR antibodies labeled multivesicular bodies (MVBs) on thin sections prepared from high-pressure frozen/freeze substituted samples, and the enlarged PVCs also were identified as MVBs. MVBs were further purified from BY-2 cells and found to contain VSR proteins via immunogold negative staining. Similar to YFP-labeled Golgi stacks, YFP-labeled PVCs are mobile organelles in BY-2 cells. Thus, we have unequivocally identified MVBs as PVCs in *N. tabacum* BY-2 cells. Uptake studies with the styryl dye FM4-64 strongly indicate that PVCs also lie on the endocytic pathway of BY-2 cells.

## INTRODUCTION

All eukaryotic cells possess a lytic compartment, characterized by the presence of acid hydrolases. In mammalian cells, this organelle is termed the lysosome, and in yeasts and plants, it is termed the vacuole. Intracellular transport of these hydrolytic enzymes occurs via the Golgi apparatus, where they are sorted from secretory proteins (Barr, 2002; Graham and Nothwehr, 2002; Jiang and Rogers, 2003; Robinson and Ritzenthaler, 2003). In all three cell types, strong evidence exists for the existence of a compartment intermediate between the *trans*-Golgi network (TGN) and the lytic compartment, which is termed the prelysosomal compartment (PLC) or the prevacuolar compartment (PVC; Lemmon and Traub, 2000; Robinson et al., 2000; Luzio et al., 2003). In mammals, mannosyl 6-phosphate receptors (MPRs) function in recruiting acid hydrolases at the TGN, from which clathrin-coated vesicles (CCVs) deliver the receptor–ligand complex to either early or late endosomes (Ghosh et al., 2003). As a result of the low pH in these compartments, the hydrolases dissociate from the MPR and are returned to the TGN

for additional rounds of sorting. The hydrolases reach the lysosome by fusion with the late endosome/PLC (Luzio et al., 2000). Collection of MPR–ligand complexes into TGN-derived CCV is mediated by tetrameric AP-1 adaptor complexes (Boehm and Bonifacio, 2001) and monomeric Golgi-localized,  $\gamma$ -ear-containing, ARF binding (GGA) proteins (Puertollano et al., 2001) and requires ADP-ribosylation factor 1 (Arf1). An analogous sorting system in yeast cells also has been described, with the sorting receptor Vps10p cycling between the Golgi apparatus and the PVC (Conibear and Stevens, 1998; Gerrard et al., 2000a, 2000b).

In plants, protein sorting in the secretory pathway is more complicated because two separate pathways diverge from the Golgi apparatus to two different vacuole destinations (Hinz and Herman, 2003; Jiang and Rogers, 2003). Plant cells possess a lytic vacuole with an acidic pH comparable to the mammalian lysosome and the vacuole of yeast cells, but they also have the capacity to store proteins in specialized vacuoles termed protein storage vacuoles (PSVs; Okita and Rogers, 1996; Jiang et al., 2001). Targeting to lytic vacuoles appears to be mediated by an integral membrane protein termed BP-80/AtELP (binding protein 80 kD, Arabidopsis epidermal growth factor-like protein), which has been shown to recognize the NPIR motif at the N terminus of aleurain and the vegetative storage protein sporamin (Ahmed et al., 1997; Paris et al., 1997). However, BP-80 also is known to bind to the C-terminal propeptide of 2S albumin, which lacks the NPIR motif (Kirsch et al., 1996). BP-80 is a member of a family of membrane proteins termed vacuolar sorting receptors (VSRs; Paris et al., 1997; Shimada et al., 1997; Hadlington and Denecke

<sup>1</sup>To whom correspondence should be addressed. E-mail ljiang@cuhk.edu.hk; fax 852-2603-5646.

The author responsible for distribution of materials integral to the findings presented in this article in accordance with the policy described in the Instructions for Authors (www.plantcell.org) is: Liwen Jiang (ljiang@cuhk.edu.hk).

<sup>W</sup>Online version contains Web-only data.

Article, publication date, and citation information can be found at www.plantcell.org/cgi/doi/10.1105/tpc.019703.

2000; Paris and Neuhaus, 2002), whose function has been confirmed both *in vitro* (Cao et al., 2000) and *in vivo* using a yeast expression system (Humair et al., 2001). Targeting determinants also have been identified for proteins sorted into the PSV (Frigerio et al., 1998; Neuhaus and Rogers, 1998). Some are located at the C terminus, but in other cases (e.g., legumin), considerable portions of the primary structure are necessary for correct delivery to the PSV (Saalbach et al., 1991). Moreover, it would appear that an aggregation/condensation process that begins in the *cis*-Golgi is part of the sorting process in legume cotyledons (Robinson and Hinz, 1999; Hillmer et al., 2001). Corresponding receptors remain to be identified, although recent data using T-DNA insertional knock-out technology implicates an Arabidopsis (*Arabidopsis thaliana*) BP-80 homolog in storage protein targeting (Shimada et al., 2004). The subcellular localization of VSR proteins has mainly been performed using immunogold electron microscopy and subcellular fractionation. Studies using these two approaches have shown that VSR proteins are not present at the tonoplast (Ahmed et al., 1997, 2000; Paris et al., 1997; Sanderfoot et al., 1998; Hinz et al., 1999). Instead, immunogold electron microscopy (immunoEM) has shown that BP-80 localizes to the Golgi apparatus and to a presumptive lytic PVC of ~250 nm in diameter in *Pisum sativum* (pea) root tip cells (Paris et al., 1997). Similarly, AtELP, the BP-80 homolog from Arabidopsis, has been located to the Golgi apparatus and a putative PVC of ~100 nm in diameter in Arabidopsis root tip cells (Sanderfoot et al., 1998). Using subcellular fractionation, BP-80 was found to partially cofractionate with Golgi membranes from *P. sativum* cotyledon cells (Hinz et al., 1999). The same result was obtained with AtELP in both wild-type (Ahmed et al., 1997; Sanderfoot et al., 1998) and transgenic Arabidopsis plants expressing a mammalian Golgi enzyme, alpha-2,6-sialyltransferase (Wee et al., 1998). However, AtELP also cofractionates in sucrose density gradients of Arabidopsis root membranes with AtSYP21, the plant homolog of the yeast PVC t-SNARE (Conceição et al., 1997). This protein functionally complements the yeast Pep12 mutant (Bassham et al., 1995) and has been localized to a putative plant PVC by immunoEM (Sanderfoot et al., 1998). Taken together, these results would suggest that VSR proteins are localized to both the Golgi apparatus and a putative post-Golgi PVC in plant cells.

Candidate PVCs for PSVs also have been identified. In developing *P. sativum* seeds, multivesicular bodies (MVBs), ranging in size from 0.5 to several  $\mu\text{m}$  and containing storage proteins have been postulated as PVCs for PSVs (Robinson et al., 1998; Robinson and Hinz, 1999). In developing *Cucurbita maxima* (pumpkin) seeds, so-called precursor-accumulating vesicles with a diameter of <0.5  $\mu\text{m}$  may serve as PVCs for endoplasmic reticulum (ER)-derived storage proteins, which bypass the Golgi apparatus (Hara-Nishimura et al., 1998). Similarly, organelles ~0.5 to 1  $\mu\text{m}$  in diameter that are labeled by antibodies generated against the tonoplast intrinsic protein isoform dark intrinsic protein (Culianez-Macia and Martin, 1993) may serve as PVCs for PSVs in developing *Nicotiana tabacum* (tobacco) seeds (Jiang et al., 2000).

Recently, we used confocal immunofluorescence microscopy to address the questions related to the relative abundance of VSR proteins in different cell compartments and their utility as

markers for these compartments (Li et al., 2002). We took advantage of the availability of several antibody preparations that recognize BP-80 and its homologs (Paris et al., 1997; Jiang and Rogers, 1998; Cao et al., 2000). Such an approach is based on the principle that labeling of a particular organelle with two or more completely different antibodies that recognize different epitopes of the same protein provides strong evidence for the presence of that protein in the organelle. In this way, we were able to demonstrate that organelles labeled by VSR antibodies are >90% separate from the Golgi apparatus and stain positively with AtSYP21 antibodies in confocal immunofluorescence (Li et al., 2002).

Because it would appear that VSRs are concentrated in PVCs (Li et al., 2002) and that the BP-80 reporter containing the BP-80 transmembrane domain (TMD) and cytoplasmic tail (CT) colocalize with endogenous VSR proteins when the reporter is expressed in transgenic *N. tabacum* culture cells (Jiang and Rogers, 1998), we surmised that the BP-80 reporter may serve as a marker for defining the lytic PVCs in plant cells. Thus, we have successfully expressed a yellow fluorescent protein (YFP)-BP-80 construct in BY-2 cells. In addition and as a control, we also have generated transgenic BY-2 cell lines expressing the Golgi marker construct GONST1-YFP (Baldwin et al., 2001). Our present confocal immunofluorescence studies demonstrate that the YFP-BP-80 reporter colocalizes with VSR-marked PVCs and is separate from the Golgi apparatus as labeled with antibodies against mannosidase I, a glycan processing enzyme residing in the *cis*-Golgi. By contrast, the GONST1-YFP construct does not colocalize with VSR-marked PVCs. We also have been able to differentiate between Golgi apparatus and the PVC on the basis of their differing sensitivities to the drugs brefeldin A (BFA) and wortmannin. Whereas BFA led to dramatic changes in the morphology of the Golgi apparatus, it had no effect on the PVC. By contrast, wortmannin had no effect on the Golgi apparatus but caused a dilation of the PVC. ImmunoEM studies on fixed cells and isolated PVCs confirmed that VSRs are concentrated in PVCs and showed that they are multivesiculate with a size of ~200 to 500 nm. Uptake studies with the styryl dye FM4-64 also strongly suggest that the PVC is an endocytic organelle. Thus, we have identified MVBs as PVCs that lie on secretory and endocytic pathways to lytic vacuoles in *N. tabacum* BY-2 cells.

## RESULTS

### New Antibodies for Detection of VSR Proteins

We previously used recombinant mannosidase I (ManI) as an antigen to raise antibodies and demonstrated that the anti-ManI immunostaining colocalized largely with both the *trans*-Golgi marker JIM84 (Satiat-Jeunemaitre and Hawes, 1992) and the *cis*-Golgi marker ManI-green fluorescent protein (GFP) fusion construct (Nebenführ et al., 1999) in immunostained transgenic *N. tabacum* BY-2 cells (Li et al., 2002). Thus, the ManI antibody seems to be a reliable marker for detecting the Golgi apparatus in BY-2 cells. In addition, we have prepared two new VSR antibodies using a truncated VSR<sub>At-1</sub> recombinant protein (lacking the TMD and CT) expressed in *Drosophila melanogaster*

S2 cells (Cao et al., 2000; Li et al., 2002) and a synthetic peptide corresponding to the BP-80 CT (Paris et al., 1997) as antigens to immunize rabbits. As shown in Figure 1, these two affinity-purified antibody preparations cross-react specifically with endogenous VSR proteins from *P. sativum*, Arabidopsis, and BY-2 cells in which a major single band at 80 kD was mainly detected in the membrane fraction (Figures 1A to 1C). Pre-immune sera did not result in detection of protein bands from these protein extracts (data not shown). When double-labeling immunofluorescence was performed in *P. sativum* root tip cells to compare these two new VSR antibodies with a known PVC marker (Arabidopsis AtSYP21) (Sanderfoot et al., 1998) and the monoclonal BP-80 antibody 14G7 (Paris et al., 1997), they mostly colocalized in punctate cytoplasmic structures (Figure 2, Table 1). These results therefore demonstrated that the two new antibodies can be used to specifically detect VSR proteins in both BY-2 cells and Arabidopsis and thus can be used as markers for defining PVCs (Li et al., 2002; Sohn et al., 2003). From now on, we will refer to these two new antibodies as anti-VSR<sub>At-1</sub> and anti-BP-80 CT.

#### Establishment of Transgenic *N. tabacum* BY-2 Cell Lines Stably Expressing YFP-BP-80 (PVC) and GONST1-YFP (Golgi) Reporters

We already have shown that the BP-80 reporter containing the BP-80 TMD and CT sequences colocalized with endogenous *N. tabacum* VSR proteins when the reporter was expressed in *N. tabacum* suspension culture cells (Jiang and Rogers, 1998). VSR proteins also are known to concentrate predominantly on PVCs (Li et al., 2002), suggesting that the BP-80 reporter might be a marker for the PVC. We therefore made a modified BP-80 reporter, in which YFP had been fused to the BP-80 TMD and CT sequences, and the resulting construct (termed YFP-BP-80 reporter) then was transferred into *N. tabacum* BY-2 cells via standard *Agrobacterium tumefaciens*-mediated transformation. As a control, we also generated transgenic *N. tabacum* BY-2 cell lines expressing GONST1-YFP as a Golgi marker (Baldwin et al., 2001). More than 20 individual transgenic BY-2 cell lines that

expressed either the YFP-BP-80 or the GONST1-YFP reporter were generated. Both reporters gave rise to typical punctate fluorescent signals in living BY-2 cells (Figure 3, panels 1 and 2).

The YFP signals detected in cells expressing the GONST1-YFP reporter were stronger than those observed in cells expressing the YFP-BP-80 reporter, presumably because the former had higher copy numbers in the transgene than the latter cell lines, as determined by DNA gel blot analysis (data not shown). Nevertheless, the various transgene copy numbers in the different transgenic cell lines did not affect the patterns of YFP signals (data not shown). Thus, we have successfully generated transgenic BY-2 cell lines expressing the two YFP reporters, and our subsequent analysis focused on two cell lines per reporter construct.

To confirm that the punctate fluorescent signals were caused by the YFP fusion proteins in both transgenic cell lines, we performed immunolabeling with GFP antibodies to detect the YFP reporters in fixed transgenic BY-2 cells expressing either the GONST1-YFP or the YFP-BP-80 fusion. As shown in Figure 3, GFP antibodies detected the two YFP fusions in confocal immunofluorescence (Figure 3, panels 3 and 4; Table 1). Most signals (>90%) detected by GFP antibodies (red) colocalized with endogenous YFP fusion proteins (green), as indicated by the appearance of yellow in the merged images.

The correct expression of the complete YFP-BP-80 reporter protein was further confirmed with protein gel blots using both GFP and BP-80 CT antibodies. As shown in Figure 4, the full-length reporter protein was mainly detected in the membrane fraction (Figure 4, lane 4, asterisk) and also was present in the vacuole fraction (Figure 4, lane 5, single asterisk). No signal was detected in wild-type cells (Figure 4, lanes 1 and 2) or in the cytosolic fraction of transgenic cells (Figure 4, lane 3). In addition, the reporter was detected in a vacuole fraction from transgenic cells (Figure 4, lane 8, asterisk) but not wild-type cells (Figure 4, lane 7) when using BP-80 CT antibodies. A protein band slightly smaller than the full-length reporter also was detected by GFP antibodies in transgenic cells expressing the YFP-BP-80 reporter (Figure 4, lane 4 and double asterisks in lanes 5 and 6). This may represent a breakdown product derived from the full-length protein, and we are not sure if this truncated protein also contributes to the fluorescent signals detected by confocal microscopy. The presence of the YFP-BP-80 reporter in the vacuole fraction is presumably attributable to the presence of PVC membranes as a contaminant because in situ the YFP-BP-80 reporter does not reach the tonoplast.

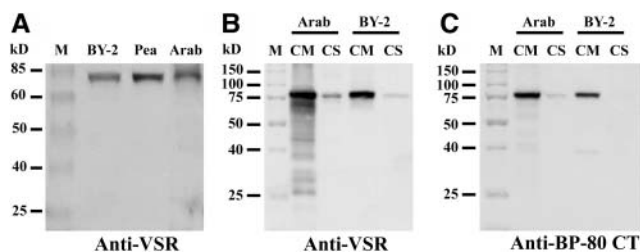


**Figure 1.** Characterization of VSR and BP-80 CT Antibodies.

**(A)** Anti-VSR detection of VSR proteins in Arabidopsis (Arab), *P. sativum* (pea), and BY-2 cells from total protein extraction.

**(B)** and **(C)** Anti-VSR and anti-BP-80 CT detection of VSR proteins from soluble (CS) and membrane (CM) fractions in BY-2 cells and Arabidopsis, respectively.

M, molecular marker in kilodaltons.

#### Confocal Laser Scanning Microscope Immunostaining Confirms the Golgi Localization of GONST1-YFP and the PVC Localization of YFP-BP-80 Reporters

To further demonstrate that the YFP-BP-80 reporter is spatially distinct from the Golgi marker GONST1-YFP, we performed immunostaining with either VSR, Man1, or AtSYP21 antibodies and compared this with either the YFP-BP-80 or the GONST1-YFP fusion protein (Figure 5). When VSR antibodies were used to label cells expressing the YFP-BP-80 reporter, >90% of the YFP signals corresponding to the reporter (green)

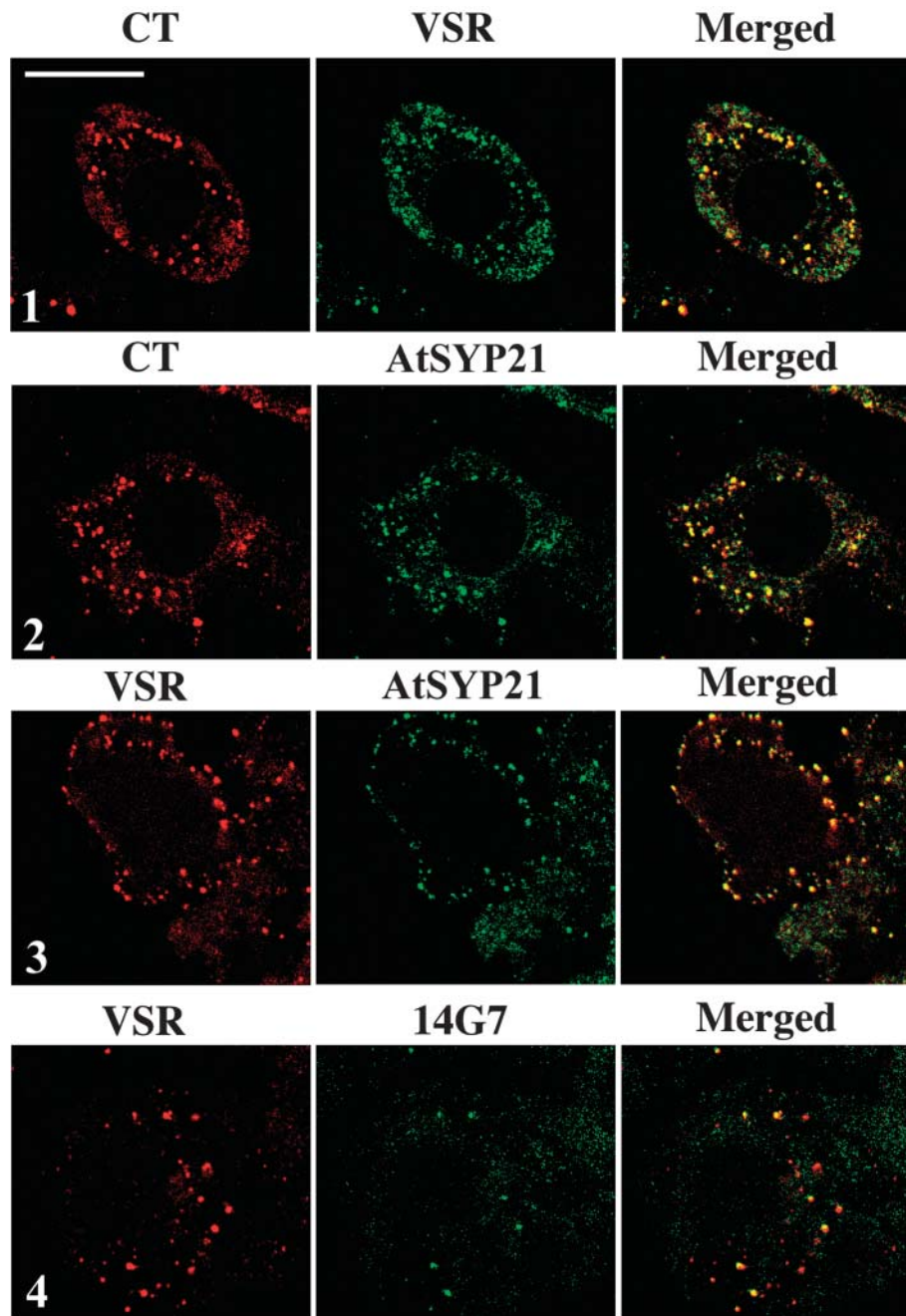


**Figure 2.** Colocalization of VSR Antibodies with PVC Markers.

Shown are double-labeling of VSR antibodies with other known PVC markers, AtSYP21 and 14G7, in fixed *P. sativum* root tip cells. The yellow appearance in the merged images indicates colocalization of two antibodies. Bar = 10  $\mu\text{m}$ .

colocalized with signals detected by VSR antibodies (red) (Figure 5, panel 1, arrowheads; Table 1). By contrast, the GONST1-YFP reporters (green) were largely separated from VSR proteins (red) in cells expressing the GONST1-YFP reporter (Figure 5, panel 2; Table 1). Similarly, when another known PVC marker, AtSYP21,

was used to compare with these two cell lines, AtSYP21 largely colocalized with the YFP-BP-80 reporter proteins but was mostly separated from the GONST1-YFP reporter (Figure 5, panels 3 and 4; Table 1). However, when Man1 antibodies were used to identify Golgi organelles and were compared with these two

**Table 1.** Quantitation of Antibody Colocalization in Confocal Immunofluorescence Images

Antibodies Compared	Percentage of Colocalization (Mean $\pm$ SD)	<i>n</i>
VSR antibodies versus AtSYP21 versus 14G7 antibodies (Figure 2)		
VSR:CT and VSR:14G7	94 $\pm$ 6	12
VSR:AtSYP21 and CT:AtSYP21	91 $\pm$ 6	15
YFP reporters versus anti-GFP in transgenic BY-2 cells (Figure 3)		
GONST1-YFP:anti-GFP	93 $\pm$ 6	23
YFP-BP-80:anti-GFP	96 $\pm$ 3	18
YFP reporters versus anti-VSR in transgenic BY-2 cells (Figure 5, panels 1 and 2)		
YFP-BP-80:anti-VSR	97 $\pm$ 3	9
GONST1-YFP:anti-VSR	8 $\pm$ 2	15
YFP reporters versus AtSYP21 in transgenic BY-2 cells (Figure 5, panels 3 and 4)		
YFP-BP-80:anti-AtSYP21	83 $\pm$ 2	6
GONST1-YFP:anti-AtSYP21	2 $\pm$ 3	11
YFP reporters versus anti-ManI in transgenic BY-2 cells (Figure 5, panels 5 and 6)		
YFP-BP-80:anti-ManI	4 $\pm$ 3	10
GONST1-YFP:anti-ManI	91 $\pm$ 4	14
YFP reporters versus anti-VSR in transgenic BY-2 cells treated with wortmannin (33 $\mu$ M) for 3 h (Figure 8C)		
YFP-BP-80:anti-VSR	85 $\pm$ 5	10
YFP reporters versus FM4-64-labeled PVCs (Figure 14)		
YFP-BP-80:FM4-64	85 $\pm$ 4	19
GONST1-YFP:FM4-64	11 $\pm$ 4	25

YFP reporters in transgenic BY-2 cells were studied by confocal immunofluorescence localization. Antibody marker for YFP was anti-GFP; antibody marker for Golgi was anti-ManI; and antibody marker for VSR protein and PVC was anti-VSR. FM4-64 is a fluorescent dye that labels prevacuolarly after endocytosis. Quantitation of the extent of colocalization for the two antibodies (or proteins) was performed from one direction only (i.e., to determine how much of the YFP-BP-80 reporter proteins colocalized with anti-VSR and not the other way around) as described previously (Jiang and Rogers, 1998). Percentage of colocalization is expressed as the mean  $\pm$  SD for the number of cells analyzed (*n*). Also, a *t* test was performed to compare results from the individual paired assays of the two reporters expressing in BY-2 cells. The resulting *P* values for the comparison were statistically significant (*P* < 0.01).

reporter proteins in transgenic cell lines, the opposite results were obtained: >90% of the YFP-BP-80 reporter proteins (green) were separated from ManI antibodies (red) in cells expressing the BP-80 reporter (Figure 5, panel 5; Table 1), whereas >90% of the GONST1-YFP proteins (green) colocalized with ManI antibodies

(red) in cells expressing the GONST1-YFP reporter (Figure 5, panel 6; Table 1). It is worthwhile to note that not all of the structures identified by anti-VSR colocalized with the YFP-BP-80 reporter proteins (Figure 5, panel 1). This may be because there are multiple VSR isoforms that are not necessarily equally distributed in different PVC types and that the VSR antibodies used in this study may recognize more than one member of the VSR protein family in BY-2 cells. In addition, because the YFP-BP-80 reporter represents the localization of a single protein, it is likely that this reporter protein may not be present in all PVCs. We currently are performing a two-dimensional gel analysis to find out how many VSR isoforms can be detected by our VSR antibodies. Nevertheless, our manifold data leave no doubt that the YFP-BP-80 and GONST1-YFP reporters are bona fide markers for the PVC and Golgi apparatus, respectively, in *N. tabacum* BY-2 cells.

### ImmunoEM Reveals the Identity of the PVC

Having established that high concentrations of VSRs are characteristic for the PVC, we initiated immunoEM studies to identify the morphology of the PVC. Despite considerable effort, we were unable to obtain adequate immunogold labeling with VSR antibodies on chemically fixed BY-2 cells. When aldehyde fixation and subsequent progressive low-temperature embedding techniques were employed, even the identification of putative PVCs (MVBs) proved impossible. Because cryosectioning of BY-2 cells is at the moment technically not possible, we finally resorted to high-pressure freezing/freeze substitution. As shown in Figures 6A to 6F, VSR antibodies specifically labeled MVBs with a diameter of 200 to 500 nm. The gold particles were restricted to the outer membranes of MVBs. Label was virtually absent on other organelles except for the occasional sparse labeling of the Golgi apparatus.

### Differential Effects of BFA on the Golgi Apparatus and PVC

BFA is a drug that has been widely used in studying protein trafficking in the secretory pathways of eukaryotic cells (Sciaky et al., 1997; Nebenführ et al., 2002). Its molecular target is a Golgi-localized guanidine nucleotide exchange factor required for converting Arf1 to its GTP form (Jackson and Casanova, 2000). Attachment of Arf1p to Golgi membranes triggers recruitment of coatamer and leads to the production of COPI-coated vesicles (Scales et al., 2000; Aniento et al., 2003). In both animals and plants, inhibition of this sequence of events by BFA treatment causes the loss of membrane-bound coatamer, the prevention of COPI vesicle formation, and the resorption of *cis*-, medial-, and *trans*-Golgi cisternae into the ER (Klausner et al., 1992; Ritzenthaler et al., 2002). In contrast with many plant cell types, BY-2 cells respond to BFA at concentrations similar to those used to induce changes in the endomembrane system of animal cells and form clearly recognizable ER-Golgi hybrid structures (Ritzenthaler et al., 2002).

To confirm that BFA at 10  $\mu$ g/mL also induces the formation of ER-Golgi hybrid structures in transgenic cells expressing the two YFP reporters, we incubated them with BFA at 10  $\mu$ g/mL for

periods up to 3 h and removed samples for YFP imaging at the times indicated (Figure 7). In cells expressing the Golgi YFP reporter, structural changes were first detected 15 min after BFA addition (Figure 7A). Enlarged fluorescent compartments were observed after 30 min and remained so for up to 3 h after BFA treatment (Figure 7A, arrows). These results are basically consistent with previously published data on BY-2 cells using Man1-GFP as a Golgi marker (Ritzenthaler et al., 2002). By contrast, when the same concentration of BFA was used to incubate BY-2 cells expressing the PVC-YFP reporter under the same conditions, no enlarged BFA compartment was detected throughout the 3-h treatment period (Figure 7B).

### Wortmannin Is without Effect on the Golgi Apparatus but Causes the PVC to Dilate

Wortmannin selectively targets the prelysosomal/endosomal compartments in mammalian cells (Bright et al., 2001), and there is evidence that this drug also blocks the trafficking of some vacuolar proteins in plant cells (Matsuoka et al., 1995; Di Sansebastiano et al., 1998). It is therefore possible that the effects of wortmannin in plants also may be localized to the PVC.

To test for this, we treated our transgenic cell lines with various concentrations of wortmannin (0 to 99  $\mu\text{M}$ ) for 3 h before confocal laser scanning microscopy imaging. As shown in Figure 8A, in cells expressing the Golgi reporter, the sizes and shapes of the YFP-labeled Golgi stacks remained unchanged at all wortmannin concentrations. In cells expressing the PVC reporter, the sizes of YFP-labeled PVCs also remained unchanged at wortmannin concentrations of  $<8.25 \mu\text{M}$  throughout the 3-h incubation period (Figure 8B). However, when the cells were treated for 3 h with wortmannin at concentrations between 16.5 and 33  $\mu\text{M}$ , the sizes of the YFP-labeled PVCs increased and appeared as small vacuoles (Figure 8B, arrows and insets). When cells were treated with wortmannin at even higher concentrations (66 and 99  $\mu\text{M}$ ), enlarged YFP-marked PVCs were not detected, and most YFP-marked PVCs disappeared (Figure 8B), which is a result that is different from its effect on the Golgi apparatus (Figure 8A).

To confirm the PVC identity of the wortmannin-induced vacuoles, we incubated cells expressing the YFP-PVC reporter with 33  $\mu\text{M}$  wortmannin for 3 h and then processed them for immunolabeling with VSR antibodies. As shown in Figure 8C (red arrows), anti-VSR labeled small vacuolar structures, a pattern

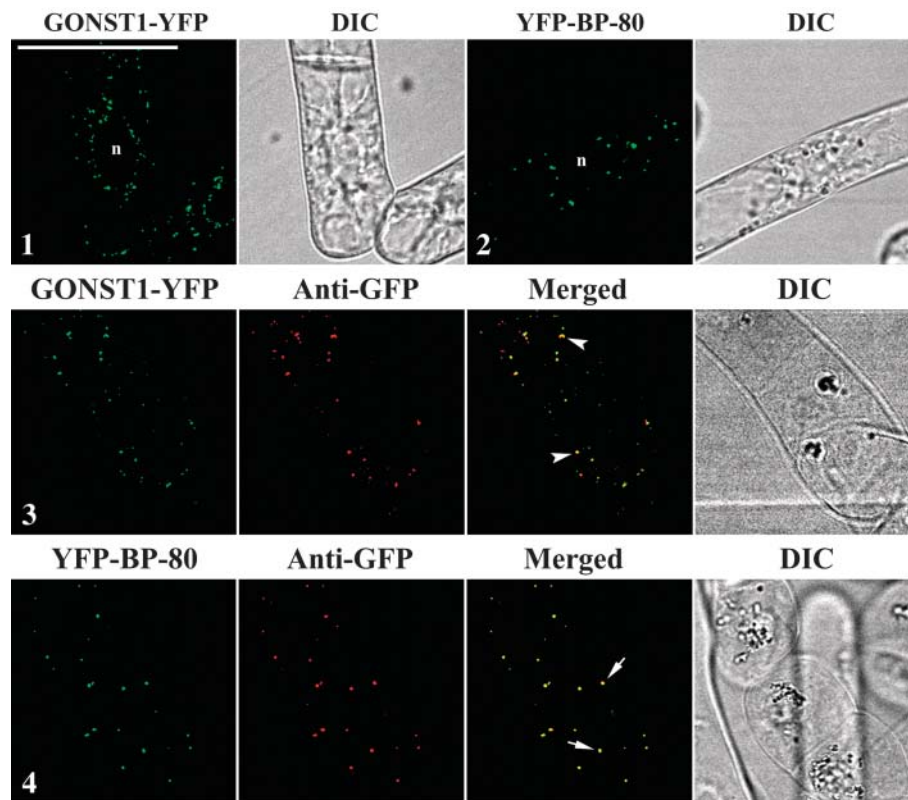


**Figure 3.** Development of Transgenic BY-2 Cell Lines Expressing the YFP-BP-80 and GONST1-YFP Reporters.

Confocal images collected from living cells expressing the Golgi marker GONST1-YFP (panel 1) and the PVC marker YFP-BP-80 (panel 2), showing similar punctate patterns. Panels 3 and 4 showed colocalization between YFP signals derived either from YFP reporters (green) or anti-GFP signals (red) in fixed cells. Colocalization of two signals was indicated by a yellow color. Arrowheads and arrows indicate colocalization (panels 3 to 4) of two signals. n, nucleus; DIC, differential interference contrast. Bar = 50  $\mu\text{m}$ .

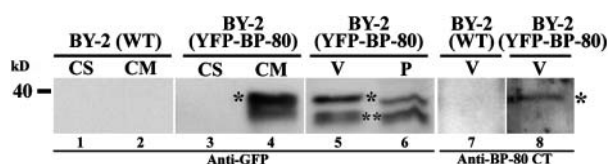


**Figure 4.** Protein Gel Blot Analysis of Transgenic BY-2 Cells Expressing the YFP-BP-80 Reporter.

Lanes 3 to 6, anti-GFP detection of the full-length YFP-BP-80 reporter proteins in membrane (CM) fraction (lane 4, asterisk) and vacuole fraction (V) (lane 5, asterisk); lane 8, anti-BP-80 CT detection of the YFP-BP-80 reporter (asterisk) in vacuole fraction. The tentative degradation products derived from the reporter proteins are indicated by double asterisks (lanes 5 and 6). Wild-type proteins also were included as controls (lanes 1 and 2). CS, soluble fraction; P, pellet.

completely different to the punctate patterns in untreated cells. These VSR-labeled vacuoles colocalized exactly with the enlarged YFP-labeled PVCs (green), as indicated by the yellow color in the merged image. Thus, wortmannin specifically causes PVCs to swell, an effect that has enabled us to show that VSRs are localized to the boundary membrane of this organelle rather than to its interior.

To investigate further the nature of the response of PVCs to wortmannin, we performed a time-course experiment with wortmannin at 33  $\mu$ M. As shown in Figure 9A, in cells expressing the YFP-Golgi marker, the Golgi stacks remained unchanged throughout the time of the wortmannin treatment, a result consistent with that shown in Figure 8A. By contrast, in cells expressing the YFP-PVC marker, enlarged YFP-labeled PVCs were first detected 30 min after the addition of wortmannin and then increased in size for the next 15 min but remained unchanged thereafter up to 3 h (Figure 9B). Similar results were obtained when wortmannin at 16.5  $\mu$ M was used (data not shown). These results confirm that the Golgi apparatus and PVC have different sensitivities to the drug wortmannin.

#### Ultrastructure of Golgi and PVCs in BFA- and Wortmannin-Treated Cells

To gain more insight into the differential responses of the Golgi apparatus and the PVC to BFA and wortmannin, an analysis of their ultrastructure was performed (Figure 10). The stably transformed GONST1-YFP cell line responded to BFA in a similar but not identical manner to wild-type BY-2 cells (see Ritzenhaller et al., 2002). First, however, and for reasons that remain unclear, Golgi stacks in the GONST1-YFP cell line have an increased number of cisternae per stack (average of 8 compared with 5 in the wild type). Their morphology is otherwise identical to Golgi stacks in wild-type cells, including the unusual feature that intercisternal filaments were detectable throughout the stack (Figure 10A). This could be because of the overexpression of the *trans*-localized GONST1-YFP in the Golgi apparatus of transgenic cells. Curiously, treatment of GONST-YFP cells for 1 h with 10  $\mu$ g/mL of BFA did not give rise to the extensive ER-Golgi

hybrid structures that were typical of wild-type cells under these conditions (Ritzenhaller et al., 2002). Instead, smaller ER-Golgi hybrid structures were found in which two to three *trans*-like cisternae were seen sandwiched between two ER-like cisternae (Figure 10B). Such structures were typically present in wild-type cells after a 10- to 20-min treatment with 10  $\mu$ g/mL of BFA. In contrast with wild-type cells, Golgi stacks of GONST1-YFP cells showed a preferred tendency to curl up, forming cup-shaped structures (Figures 10C and 10D), and to fuse with one another, producing aggregates (Figure 10E). BFA had no apparent effect on the morphology of MVBs (Figure 10E, arrow).

The application of wortmannin (at 33  $\mu$ M for 1 h) to GONST1-YFP BY-2 cells did not cause any change in the size or morphology of the Golgi apparatus: individual Golgi stacks were indistinguishable between control and treated cells (Figures 11A and 11F). The only organelle that showed any noticeable response to wortmannin was the MVB. In untreated cells, these roughly spherical structures have a diameter of 300 to 400 nm and are therefore somewhat smaller than Golgi stacks (Figures 11B and 11C). Depending on the plane of section, they are frequently seen to have a thick osmiophilic plaque on their cytosolic surface (Figures 11D and 11E). The numerous microvesicles in the interior of the MVB had an average diameter of 70 nm. After wortmannin treatment, MVB as seen in control cells was no longer detected in the GONST1-YFP cells. Instead, small vacuoles (diameter 500 to 800 nm) were seen (Figures 11G and 11H, chevrons), each with a small number of 70-nm microvesicles. These results are consistent with the confocal observation that the YFP-BP-80-marked PVCs were induced to form small vacuoles after wortmannin treatments (Figures 8B, 8C, and 9B).

#### Isolation of PVCs

To confirm the specificity of VSR labeling, we attempted to isolate VSR-enriched fractions and to examine them for the presence of MVBs. We first prepared and identified crude fractions enriched in VSR proteins using a discontinuous sucrose gradient followed by protein gel blotting using VSR antibodies (Figure 12A). The fractions containing the most VSR proteins (Figure 12A, fractions 6 to 10) were further subjected to isopycnic centrifugation on a continuous sucrose density gradient that was probed with various marker antibodies. As shown in Figure 12B, fractions 10 to 12 contained little Golgi Man1 and plasma membrane ATPase but showed high concentrations of VSR proteins. To emphasize this enrichment of VSR proteins in the gradient fractions, we present a protein gel blot with equal amounts of protein per lane that shows total proteins from a BY-2 cell extract (Figure 12C, lane 1), VSR-enriched protein from fractions of 6 to 8 in Figure 12A (Figure 12C, lane 2), and fraction 11 from the experiment shown in Figure 12B (Figure 12C, lane 3). Fraction 11 of the sucrose density gradient was therefore processed for immunoEM. As shown in Figure 13, fraction 11 contained numerous circular membranous structures  $\sim$ 200 to 500 nm in size that resembled MVBs (Figure 13A) and labeled positively with VSR antibodies in immunogold negative staining (Figures 13B to 13E). This labeling was specific for VSR antibodies because neither  $\alpha$ -TIP antibodies (an unrelated PSV protein) nor secondary



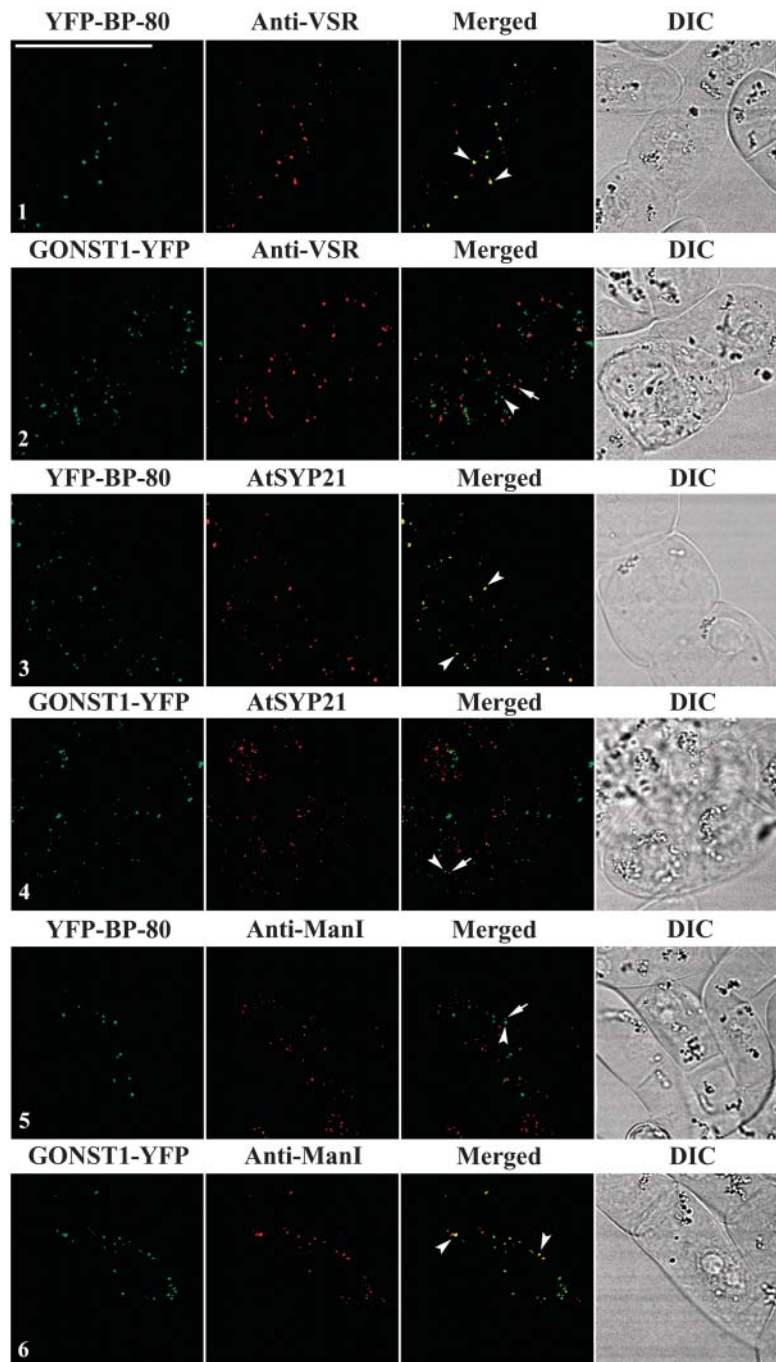


**Figure 5.** Anti-VSR Colocalizes with the YFP-BP-80 Reporter but Is Separate from the GONST1-YFP Reporter.

Transgenic *N. tabacum* BY-2 cells expressing either YFP-BP-80 or GONST1-YFP reporters were fixed and incubated with either VSR, AtSRY21, or ManI antibodies to detect PVC and Golgi stacks, respectively. The primary antibodies were detected with rhodamine-conjugated secondary antibodies (red), whereas the two YFP reporters (green) were ready for detection in the confocal microscope using a 488-nm laser. When green and red images were superimposed, colocalization of two signals is indicated by a yellow color. Arrowheads and arrows indicate colocalization and separation, respectively. n, nucleus. Bar = 50  $\mu$ m.



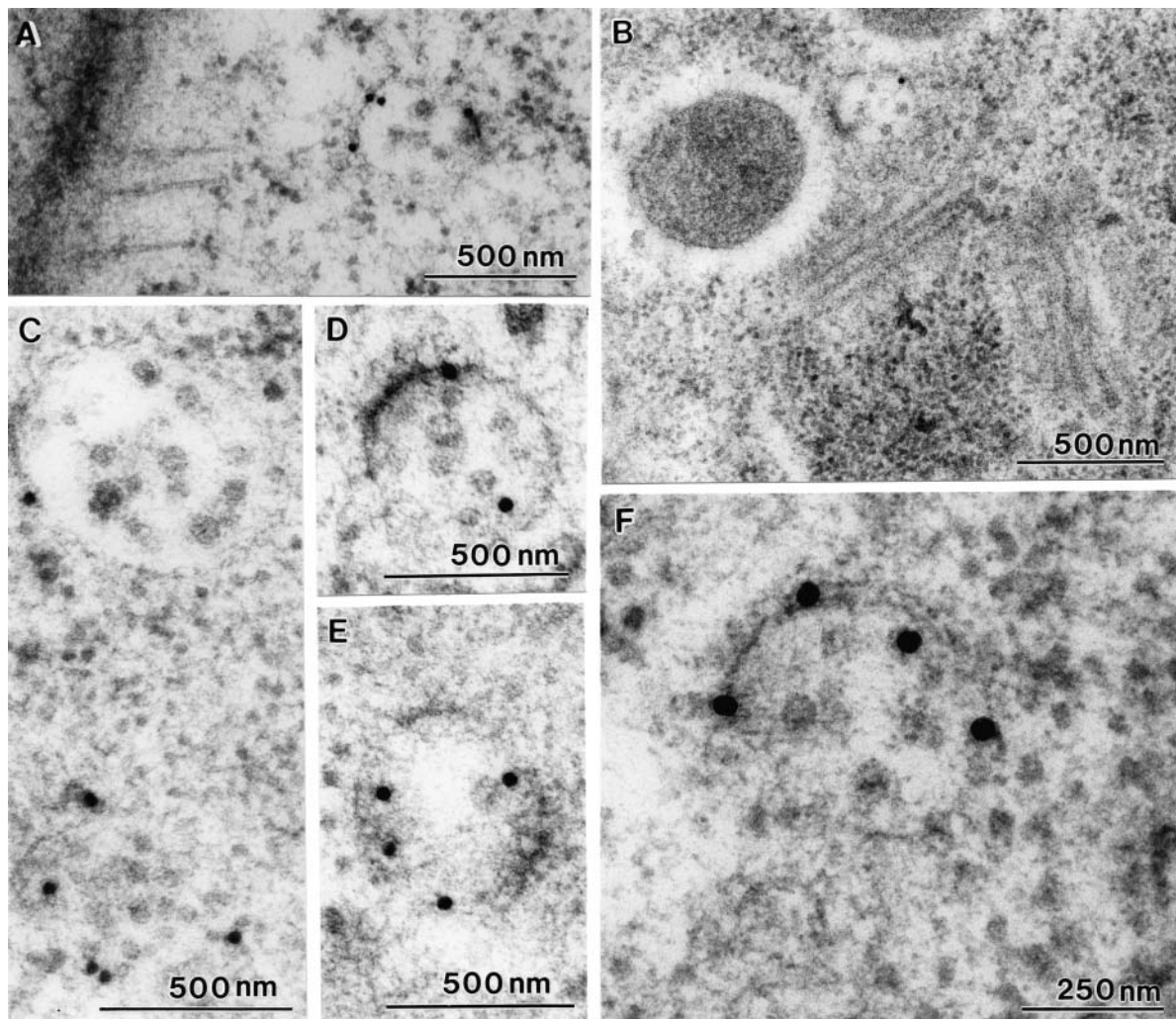


**Figure 6.** Immunogold Labeling of MVBs with VSR Antibodies.

(A) to (F) Thin sections prepared from high-pressure frozen/freeze-substituted samples were stained with VSR antibodies. Various MVBs are depicted that are labeled specifically with VSR antibodies.

antibodies alone stained these structures under the same conditions (Figures 13F and 13G). Furthermore, there was very little background labeling (data not shown). These data confirm that VSRs are concentrated on the surface of MVB-like structures.

#### FM4-64 Labels the PVC but Not the Golgi Apparatus

The fluorescent styryl dye FM4-64 has been used as an endosomal marker for endocytosis studies because after having been taken up, it passes through an endosomal/PVC on its way to the vacuole (Ueda et al., 2001; Emans et al., 2002). We therefore performed uptake studies using FM4-64 on BY-2 cells to find out if the same PVCs lie on the Golgi-derived secretory as well as endocytic pathways. Consistent with previous results, the dye remained at the cell surface of wild-

type cells during early stages of incubation but was rapidly taken up into the cells, exhibited a punctate (endosome) pattern 15 min after starting the incubation, and later labeled the tonoplast after 3 h (Figure 14, panel 1). We then repeated these experiments on our transgenic BY-2 cell lines expressing either the YFP-Golgi or YFP-PVC reporters. Fifteen to thirty minutes after incubation with FM4-64, most of the internal structures labeled by FM4-64 (red) overlapped with the YFP-PVC reporter signal (green) (Figure 14, panel 2, arrowheads; Table 1). By contrast, in cells expressing the YFP-Golgi reporter, the YFP reporter proteins (green) were largely separated from the FM4-64-labeled internal structures (red) (Figure 14, panel 3, arrow versus arrowhead; Table 1). These results indicate that the YFP-labeled PVC lies on the endocytic pathway in transgenic *N. tabacum* BY-2 cells.

### PVCs Are Mobile Organelles

Previous studies using BY-2 cells expressing a Golgi-targeted GFP-ManI fusion construct have demonstrated that Golgi stacks exhibit a stop-and-go movement in living cells (Nebenführ et al., 1999). To determine whether the YFP-labeled PVCs are also mobile in BY-2 cells, we performed live cell time-course YFP imaging for both the PVC and Golgi YFP-reporters. Most YFP-marked Golgi stacks displayed a constant movement during a period of 90 s, and some Golgi stacks even moved as far as half a cell length at a speed of 2  $\mu\text{m/s}$  (see supplemental movie A online, see arrow as an example). Similarly, many PVCs showed continual movement in living cells, and some could move across half of a cell in <15 s (see supplemental movie B online, see arrow as an example). In general, PVCs displayed three kinds of

motion: a few remained still, some moved across the cell, and a few moved vertically from the top to the bottom of the cell.

### DISCUSSION

#### VSR Proteins and Integral Membrane VSR Reporter Constructs as Markers for PVCs

In mammalian cells, MPRs traffic with cargo from the TGN (synthetic pathway: MPR46 and MPR300) and plasma membrane (endocytic pathway: MPR300 only) via CCVs to early and late endosomes (Hille-Rehfeldt, 1995; Ghosh et al., 2003). Although there are cell type-specific variations in subcellular distribution, in the majority of cells investigated, MPRs are

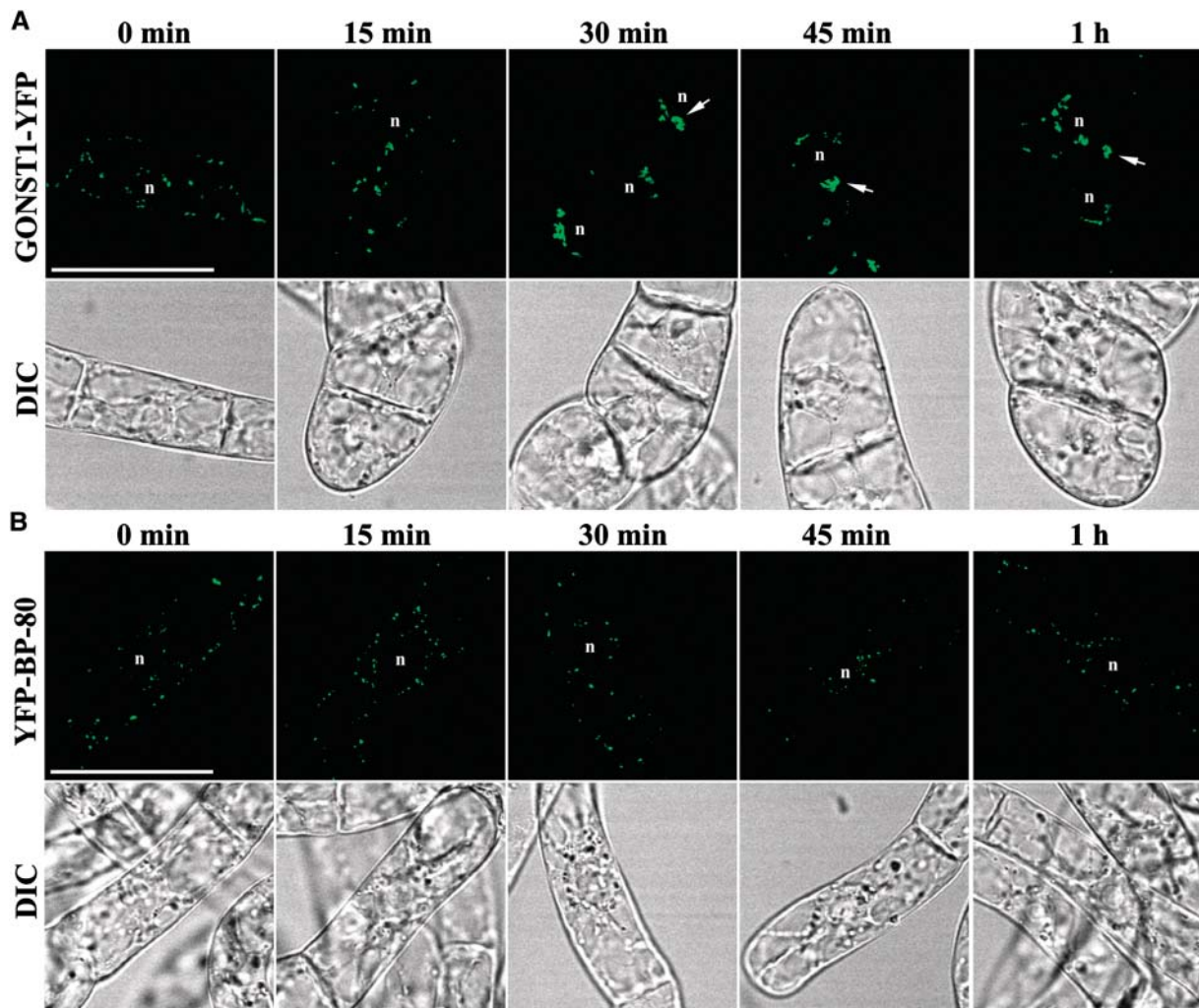


**Figure 7.** BFA at 10  $\mu\text{g/mL}$  Induces Structural Changes in YFP-Marked Golgi Stacks but Not in YFP-Marked PVCs.

Transgenic BY-2 cells expressing either the GONST1-YFP reporter (**A**) or the YFP-BP-80 reporter (**B**) were incubated with BFA at 10  $\mu\text{g/mL}$  for up to 1 h. Treated cells then were collected at the times indicated for YFP imaging in the confocal laser scanning microscope. Arrows indicate BFA-induced aggregates in cells expressing the GONST1-YFP Golgi marker. n, nucleus. Bars = 50  $\mu\text{m}$ .

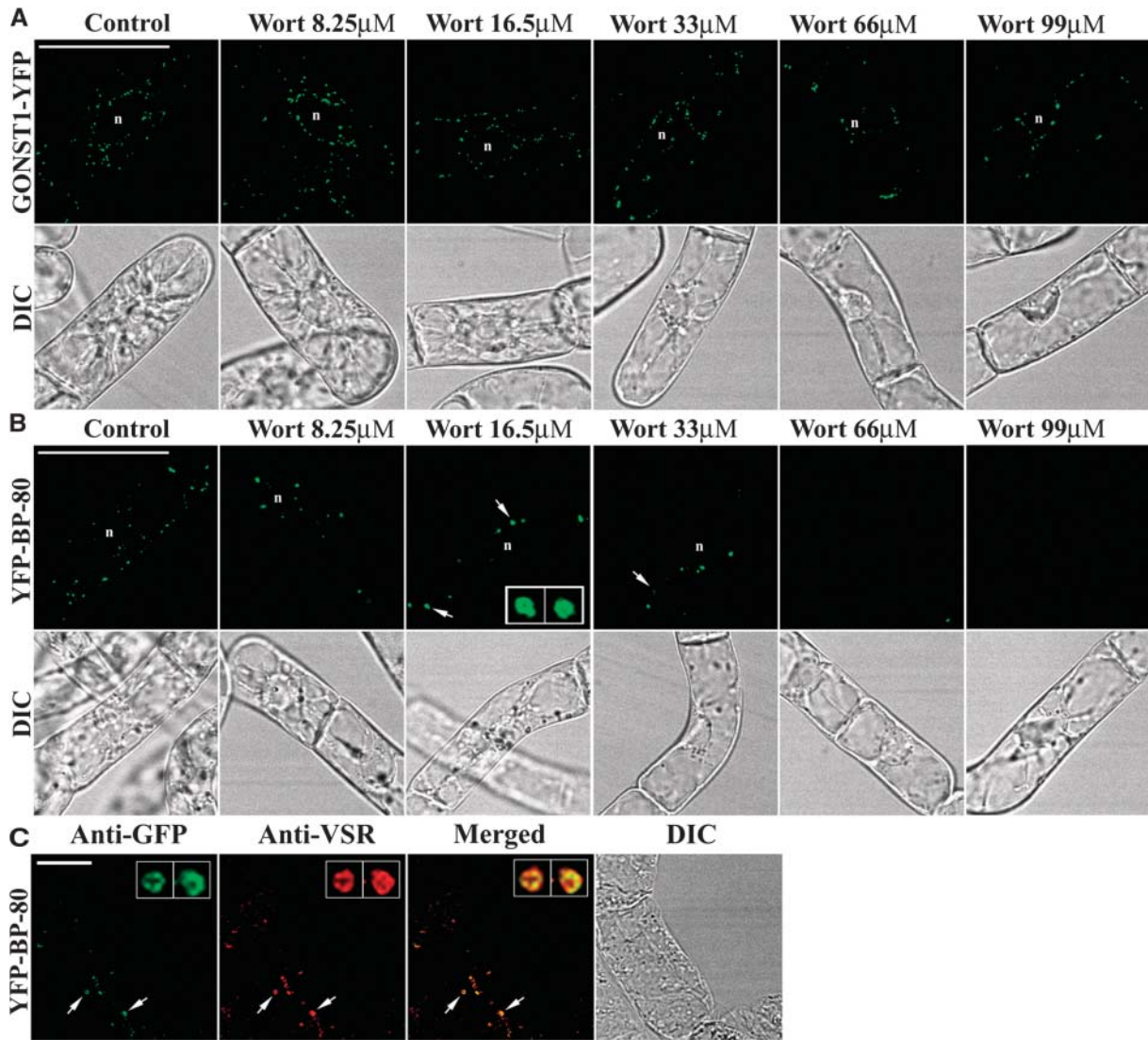


**Figure 8.** Wortmannin Induces the YFP-BP-80-Labeled PVCs to Form Small Vacuoles in a Dose-Dependent Manner.

**(A)** and **(B)** Transgenic cells expressing the Golgi **(A)** and PVC **(B)** reporters were incubated with wortmannin (Wort) at various concentrations as indicated for 3 h before the treated cells were sampled for YFP imaging. Arrows in **(B)** indicate small vacuoles derived directly from the YFP-BP-80-labeled PVCs. The insets in the third panel of **(B)** are enlarged vacuole images of the two structures indicated by the arrows.

**(C)** Colocalization of anti-VSR (red) with PVC-derived vacuoles in transgenic cells expressing the YFP-BP-80 reporter after treatment with wortmannin at 16.5  $\mu$ M for 3 h. The insets are enlarged vacuole images of the two structures indicated by the arrows.

n, nucleus. Bar in **(A)** and **(B)** = 50  $\mu$ m; bar in **(C)** = 20  $\mu$ m.

predominantly concentrated in the endocytic organelles, rather than in the TGN (cf. Griffiths et al., 1988, 1990; Hirst et al., 1998). Similarly, Vps10p, the receptor for carboxypeptidase in bakers' yeast, is transported via CCV to a multivesiculate PVC (Conibear and Stevens, 1998). Vps10p has been detected by immunofluorescence in an ultrastructurally undefined late Golgi compartment and colocalizes with Kex2p (Cooper and Stevens, 1996). However, immunogold labeling studies comparable to those performed for the MPRs are lacking.

In plants, recent confocal immunofluorescence microscopy studies have indicated that BP-80 and other VSR homologs also are predominantly located to non-Golgi PVC structures (Li et al., 2002). When a construct containing the TMD and CT sequences of BP-80, together with proaleurain as the luminal domain, was expressed in suspension-cultured *N. tabacum* cells, the BP-80 reporter successfully delivered mature aleurain into a lytic-type vacuole. Cleavage of proaleurain from the integral membrane construct and its proteolytic processing into mature aleurain took



place in a Kex2 protease-containing post-Golgi compartment (Jiang and Rogers, 1998). This compartment was therefore functionally defined as a lytic PVC. In addition, the expressed BP-80 reporter colocalized with endogenous VSR proteins in cultured *N. tabacum* cells (Jiang and Rogers, 1998).

These observations suggest that both endogenous VSR proteins and transiently expressed BP-80 reporter constructs may be used as markers to identify lytic PVCs in plant cells. To confirm this, we have generated two stable transgenic *N. tabacum* BY-2 cell lines: one expressing a YFP-BP-80 reporter construct and the other GONST1-YFP, a Golgi marker. In confirmation of our previous results obtained by transient expression on protoplasts (Jiang and Rogers, 1998), we have shown that in *N. tabacum*, BY-2 cells stably transformed with these two reporters. The YFP-BP-80 reporter rather than the GONST1-YFP reporter colocalizes with endogenous VSR proteins to a structure distinct from the Golgi apparatus. This result conforms to the notion that VSR proteins are concentrated in PVCs (Li et al., 2002) and implies that VSR proteins recycle back to the Golgi for a brief selection of transit cargo molecules before returning to the PVCs for cargo delivery.

### The PVC Lies on the Endocytic Pathway

Although still not unequivocally demonstrated, by possessing numerous clathrin-coated pits at the plasma membrane and having endosome-like structures, plants fulfill the structural requirements to perform clathrin-dependent receptor-mediated endocytosis (for a review, see Battey et al., 1999). Moreover, many plant homologs to the mammalian clathrin endocytosis machinery have been identified recently, and many plausible candidates for endocytic ligands are now under consideration (Holstein, 2002). The use of fluorescent styryl dyes has provided additional evidence for the operation of endocytosis in plants (Emans et al., 2002). Such dyes (e.g., FM4-64 and FM1-43) only fluoresce in the context of a hydrophobic lipid environment, and when added to the extracellular medium, they become incorporated into the plasma membrane where they are internalized and transported via intermediate organelles to the vacuole (Vida and Emr, 1995). Colocalization with internalized FM4-64 is therefore becoming an accepted means of ascertaining whether a particular compartment is a potential endosome in plant cells (Kim et al., 2001; Ueda et al., 2001; Bolte et al., 2004).

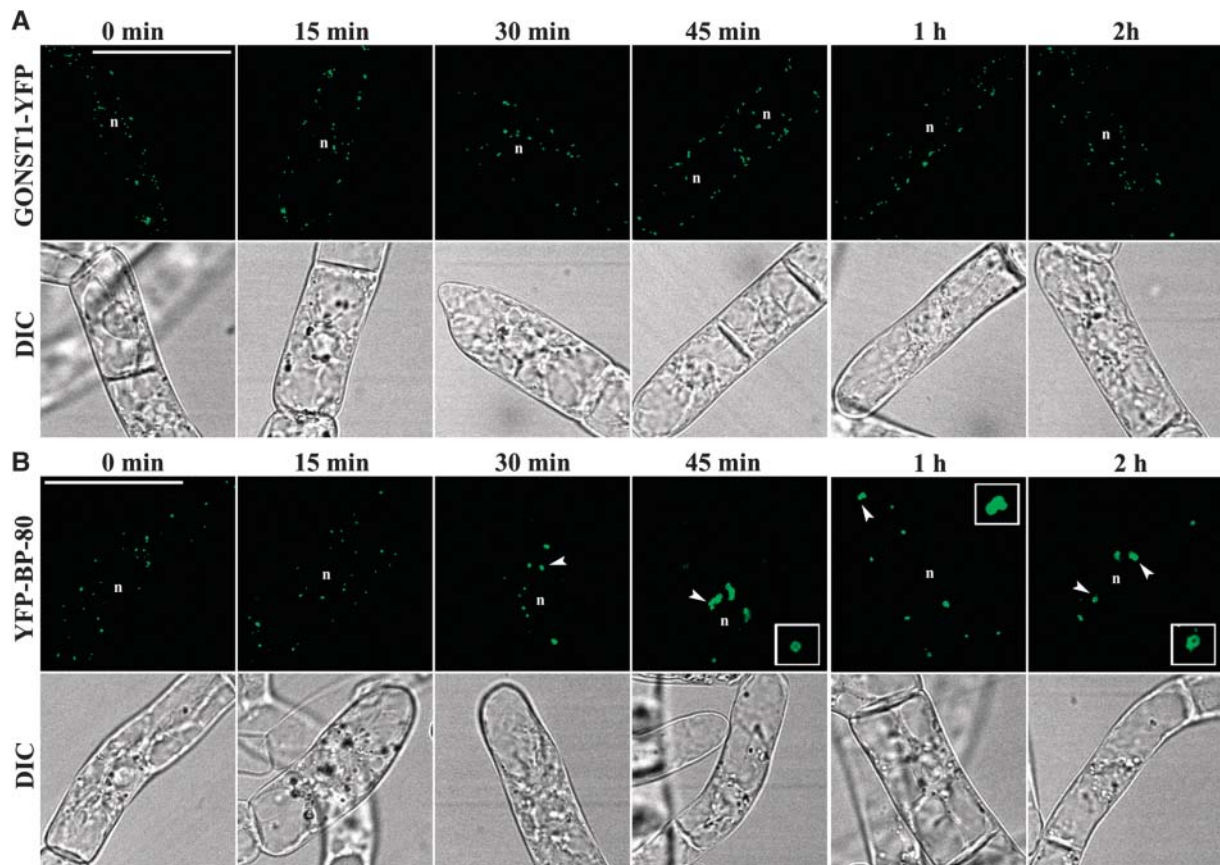


**Figure 9.** Time Course of Wortmannin-Induced PVC Vacuole Formation.

**(A)** and **(B)** Transgenic BY-2 cell lines expressing the Golgi and PVC reporters were incubated with wortmannin at 33  $\mu\text{M}$  for the times indicated. Samples of treated cells then were taken for YFP imaging. Arrowheads in **(B)** indicate wortmannin-induced vacuole formation. Insets are vacuolated YFP-BP-80-labeled PVCs. n, nucleus. Bars = 50  $\mu\text{m}$ .

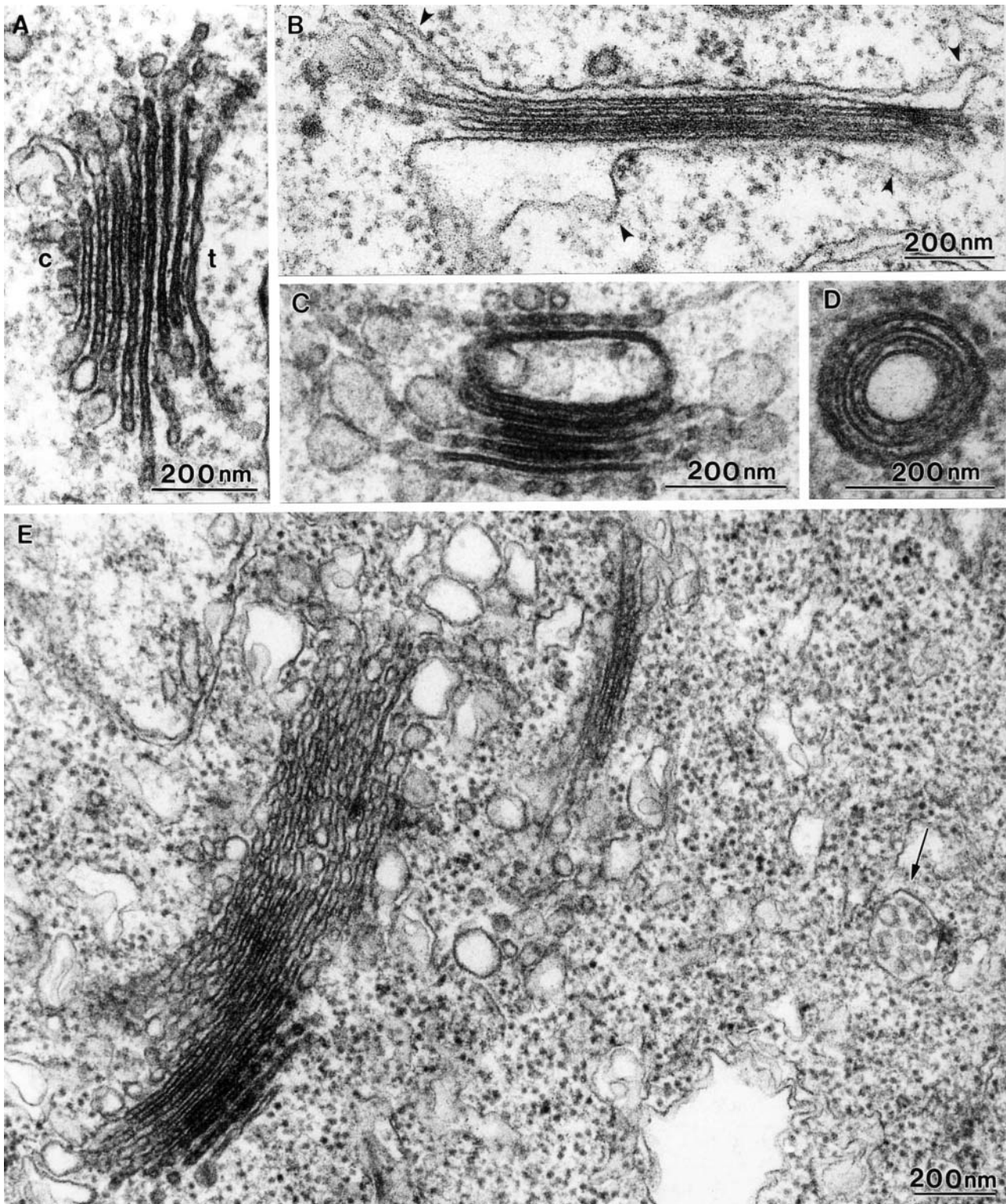


**Figure 10.** Ultrastructural Analysis of BFA on GONST1-YFP-Transformed BY-2 Cells.

(A) Golgi stack from an untreated cell. c, *cis* face; t, *trans* face.

(B) ER-Golgi hybrid. Note the outermost Golgi cisternae at both faces have an ER-like structure (arrowheads).

(C) and (D) Cup-shaped Golgi structures sectioned in different planes.

(E) Multiple Golgi stack aggregates adjacent to a multivesicular body (arrow) that has remained unchanged in size and morphology (Figure 11).

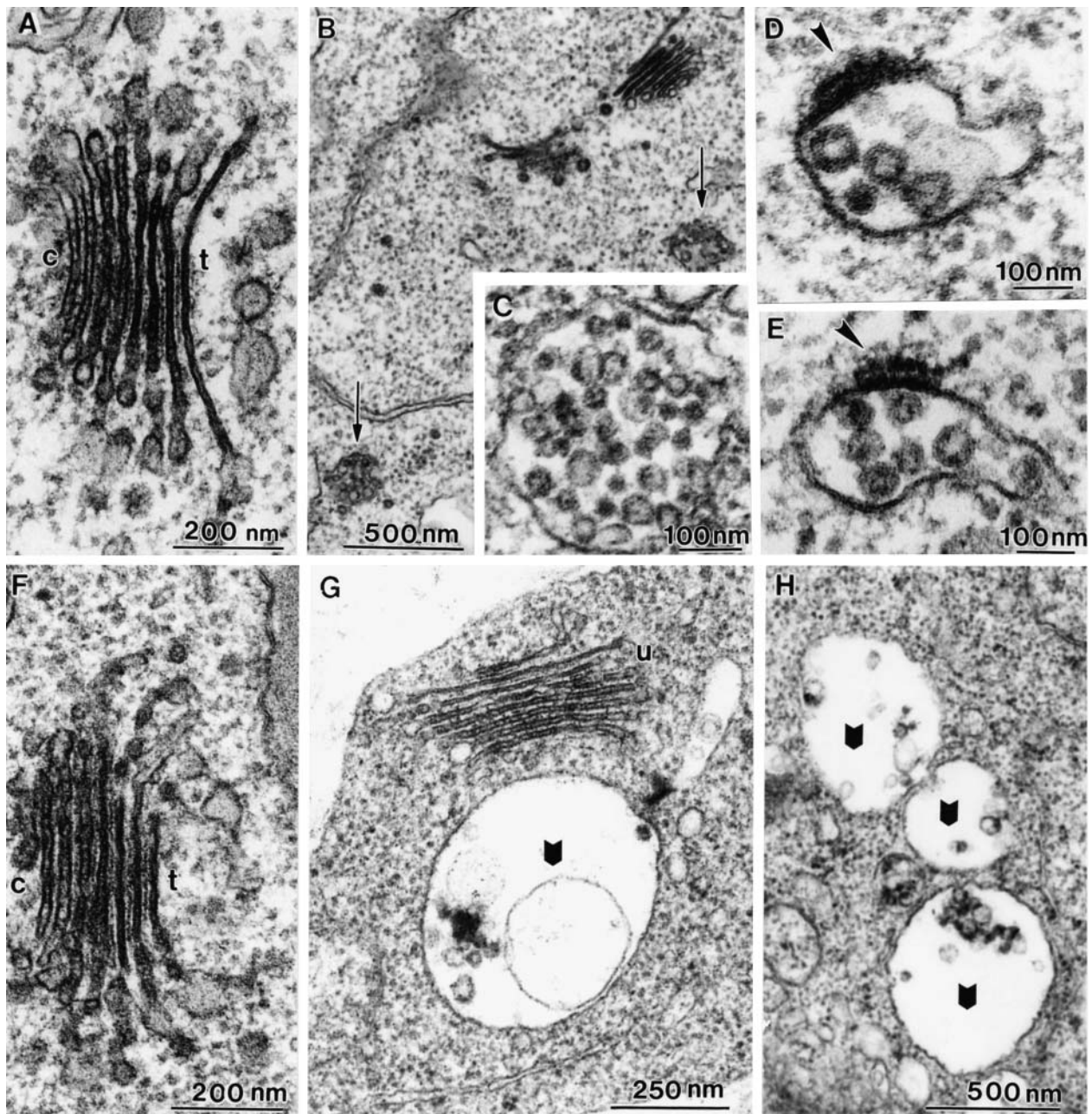


**Figure 11.** Ultrastructural Analysis of Wortmannin Effects on BY-2 Cells.

(A) Golgi stack in an untreated cell. c, *cis*-cisterna; t, *trans*-cisterna.

(B) Size comparison of Golgi stacks and MVBs (arrows) in an untreated cell.

(C) High magnification of a multivesicular body in an untreated cell.

(D) and (E) Highly stainable plaques (arrowheads) at the cytoplasmic surface of MVBs in untreated cells.

(F) Golgi stack in a cell treated with wortmannin for 1 h. Stack parameters (number of cisternae, polarity) appear unchanged.

(G) and (H) MVBs (chevrons) swell and show reduced numbers of internal vesicles in wortmannin-treated cells.



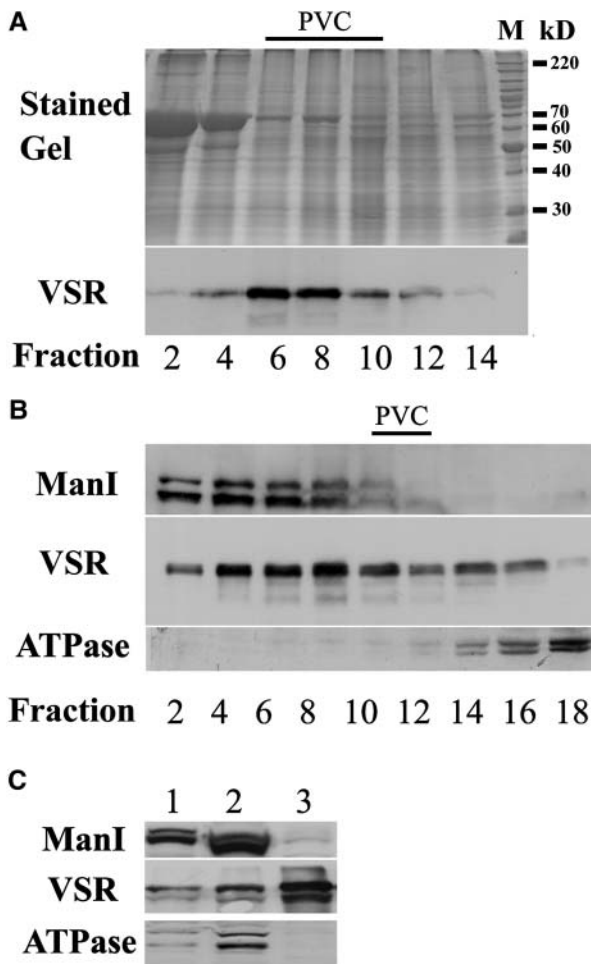


**Figure 12.** Isolation of PVCs from BY-2 Cells.

**(A)** Identification of fractions enriched in VSR proteins. Cell homogenates were layered onto a discontinuous sucrose density gradient (20 and 60% [w/w]). Fractions were collected and subjected to SDS-PAGE followed by immunodetection with VSR antibodies. M, molecular marker in kilodaltons.

**(B)** The VSR-enriched fractions from **(A)** (fractions 6 to 8) were further layered onto a continuous sucrose density gradient (25 to 50% [w/w]) and centrifuged isopycally. Fractions were collected for protein gel blotting using various antibodies.

**(C)** Progressive enrichment of VSRs in subcellular fractionation. Total protein from BY-2 cell homogenate (lane 1), VSR-enriched fractions 6 to 8 of **(A)** (lane 2), and fraction 11 from **(B)** (lane 3) were used for protein gel blot analysis using various antibodies. Equal amounts of protein (15  $\mu$ g) applied to each lane.

Recently, this technique has been employed in studies on Rab GTPases, which are well known to play critical roles in vesicle budding and fusion in mammalian cells, especially in endocytosis (Rodman and Wandlinger-Ness, 2000; Zerial and McBride, 2001). Thus, Ara6 (Rab5)-positive structures in Arabidopsis root cells have been shown to stain with FM4-64 (Ueda et al., 2001), whereas a related Rab5-bearing organelle in BY-2 cells does not (Bolte et al., 2004). In our investigation, 15 to 30 min after FM4-64

was added to BY-2 cells expressing the YFP-BP-80 reporter, nearly all of the YFP-positive organelles became stained with the dye. Because we have shown that YFP-BP-80 is a bona fide reporter for the PVC in BY-2 cells, we regard this result as convincing evidence that the PVC is also an endocytic compartment.

### PVCs Are Multivesiculate in BY-2 Cells

The biosynthetic pathway to the lytic compartment of mammalian and yeast cells converges with the degradative (endocytic) pathway at the PLC/PVC, also termed the late endosome (Conibear and Stevens, 1998; Le Borgne and Hoflack, 1998; Gu and Gruenberg, 1999; Lemmon and Traub, 2000). Discharge of the contents of the late endosome/PVC into the lysosome/vacuole appears to occur by direct fusion and then separation of the two compartments, rather than vesicle transfer (Luzio et al., 2000). The various endocytic compartments have in common their multivesiculate nature (van Deurs et al., 1993; Futter et al., 1996; Mulholland et al., 1999). These internal vesicles appear to originate by invagination in early or recycling endosomes (Parton et al., 1992). Normally, they are rapidly degraded in the lysosome/vacuole but have been shown to accumulate in the lumen of the vacuole of mutant yeast cells incapable of vacuolar acidification (Wurmser and Emr, 1998).

It has been known for some time that the internal vesicles of multivesicular endosomes in mammalian and yeast cells have a different composition than the limiting membrane (Griffiths et al., 1990; Kobayashi et al., 1998). It also is often considered that the proteins in the membrane of these vesicles are destined for degradation in the vacuole, suggesting that their sorting into the vesicle membrane must be signal mediated. Polar TMDs (Reggiori et al., 2000), di-Leu motifs (Kil et al., 1999), as well as ubiquitination (Reggiori and Pelham, 2001) all have been implicated in this process. Also involved is the coated plaque, characteristic of the surface of early endosomes (Futter et al., 1996; Raposo et al., 2001), which is structurally distinct from the clathrin buds that mediate the transport of recycling receptors (van Dam and Stoorvogel, 2002). The plaque is made up of a bilayer of clathrin triskelions but lacks the adaptor complexes AP1, AP2, and AP3 and is thought to act as a trap for downregulated receptors (Sachse et al., 2002).

MVBs, with a very similar morphology to the endosomes of mammalian cells, including plaques at their cytosolic surface, have frequently been recorded in the plant literature (for references, see Robinson and Hinz, 1999; Robinson et al., 2000). On the basis of uptake experiments with electron dense tracers, they also have been implicated in plant endocytosis (Hillmer et al., 1986; Galway et al., 1993). In addition, the cytochemical detection of acid phosphatase and peroxidase (Record and Griffing, 1988) indicates that plant MVBs lie on the transport route to the lytic vacuole. MVBs also have been proposed as being intermediates in transport to PSVs, both for simple PSVs as in legume cotyledons (Robinson et al., 2000) as well as for compound PSVs with globoid and crystalloid contents (Jiang et al., 2002). On the other hand, small vacuoles  $\sim$ 250 nm in diameter that labeled positively with VSR antibodies were

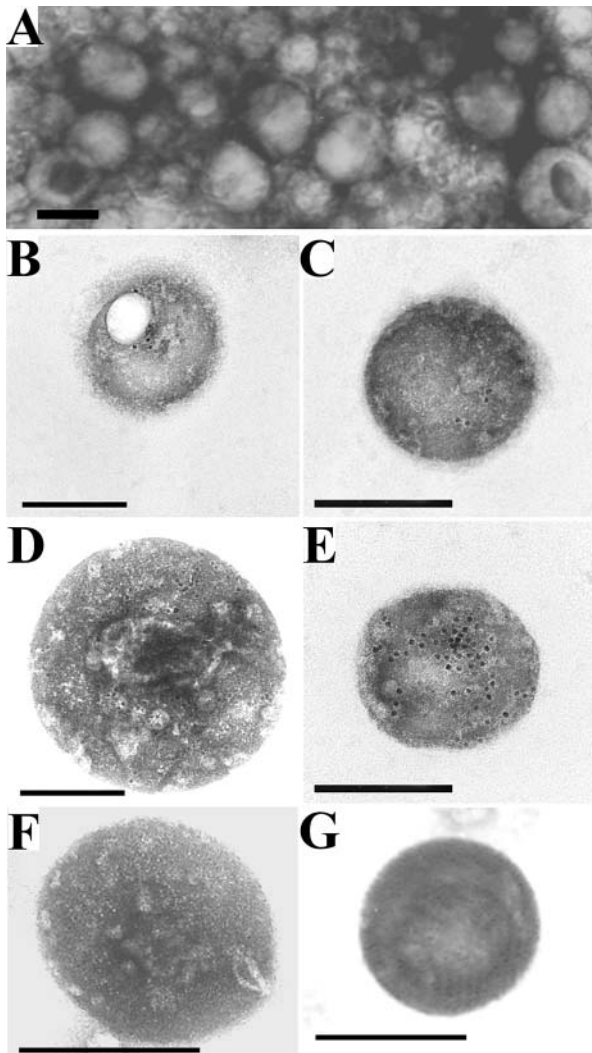


**Figure 13.** Immunogold Negative Staining of Isolated PVCs.

(A) Morphology of freshly isolated PVCs in VSR-enriched fraction 11 from Figure 12.

(B) to (E) Various PVCs after immunogold staining with VSR antibodies.

(F) and (G) Control labeling of isolated PVCs using  $\alpha$ -TIP and secondary antibodies alone, respectively.

claimed to be the lytic PVC in cells of *P. sativum* root tips (Paris et al., 1997). Conversely, in *Arabidopsis* root tip cells, clusters of tubule/vesicle-like structures  $\sim 100$  nm in diameter were described as PVCs because they labeled with both AtSYP21 and AtELP antibodies (Sanderfoot et al., 1998). However, the identification of these PVC structures as MVBs was not possible in either of these two studies.

In this investigation, through immunogold labeling of sections cut from high-pressure frozen/freeze-substituted samples, we have successfully provided clear in situ evidence that VSRs are specifically localized to MVBs. Using VSR antibodies to probe subcellular fractions for organelles in which VSRs are concentrated, we again isolated VSR-labeled membranous organelles

that were multivesiculate. Interestingly, VSR labeling is restricted to the boundary membrane rather than the internal vesicles of the MVBs, suggesting that only a small proportion of the VSRs that reach the PVC at any one time are destined for degradation.

This in part agrees with the situation in mammalian cells, but the literature with regard to MPRs in mammalian cells is more complicated. Whereas it seems that the MPR46 rapidly segregates from the MPR300 in endosomes and diffuses laterally into tubular extensions for recycling, the MPR300 becomes concentrated on the internal vesicles (Klumperman et al., 1993). However, it is incorrect to assume that as a result of this differential distribution in MPR types the MPR300 will automatically be degraded by transport of the luminal vesicles to the lysosome. Neither of the MPRs is ubiquitinated, both have similar half-lives, and both cycle between endosome and TGN or endosome and plasma membrane (Hille-Rehfeldt, 1995; Ghosh et al., 2003).

#### Wortmannin but Not BFA Targets MVBs in BY-2 Cells

BFA is an effective inhibitor of secretion in all eukaryotic cells, whose primary target is usually considered to be a Golgi-localized, Arf1-specific, GTPase-exchange factor (for review, see Nebenführ et al., 2002). The GONST1-YFP cell line responds to BFA treatment in a similar but not identical manner to wild-type BY-2 cells. Whereas BFA-induced changes in Golgi structure were observable both in the confocal laser scanning microscope and the electron microscope, MVBs inclusive of the plaque-like coat were not affected. In this respect, plants resemble mammalian cells whose MVBs also are unaffected by BFA (Sachse et al., 2002). A likely explanation for this may lie in the fact that recruitment of the adaptor complex AP1 requires Arf1, and this is absent from the plaque of MVBs (Sachse et al., 2002).

The drug wortmannin, on the other hand, interferes with lipid kinases whose phosphorylated products are important regulators of vesicle-mediated protein trafficking (Corvera et al., 1999). The best example is Vps34p, phosphatidylinositol 3-kinase (PI-3K), which is essential for protein sorting in yeast (Schu et al., 1993) and is known to bind to Cys/His-rich FYVE domains in proteins vital to vesicular transport (Gaulhier et al., 1998; Tall et al., 1999). Its substrate, phosphatidylinositol 3-phosphate, has been localized to endosomes in both mammalian and yeast cells (Gillooly et al., 2000) and has been shown to be necessary for the formation of the internal vesicles in mammalian multivesicular endosomes (Fernandez-Borja et al., 1999). Wortmannin is generally regarded as being a specific inhibitor of PI-3K (Vanhaesebroeck et al., 1997), and although it may also act as an effector of Rab5- and Rab7-GTPases (Vieira et al., 2003), it leads to a drastic reduction in the number of internal endosomal vesicles and a loss of the plaque-like coat when applied to mammalian cells (Sachse et al., 2002). In addition, wortmannin treatment causes multivesicular endosomes to swell (Reaves et al., 1996; Bright et al., 2001).

There have been several studies on plant cells in which wortmannin has been successfully employed to block transport to the vacuole (Nakamura et al., 1993; Matsuoka et al., 1995; Koide et al., 1997; Di Sansebastiano et al., 1998). Wortmannin

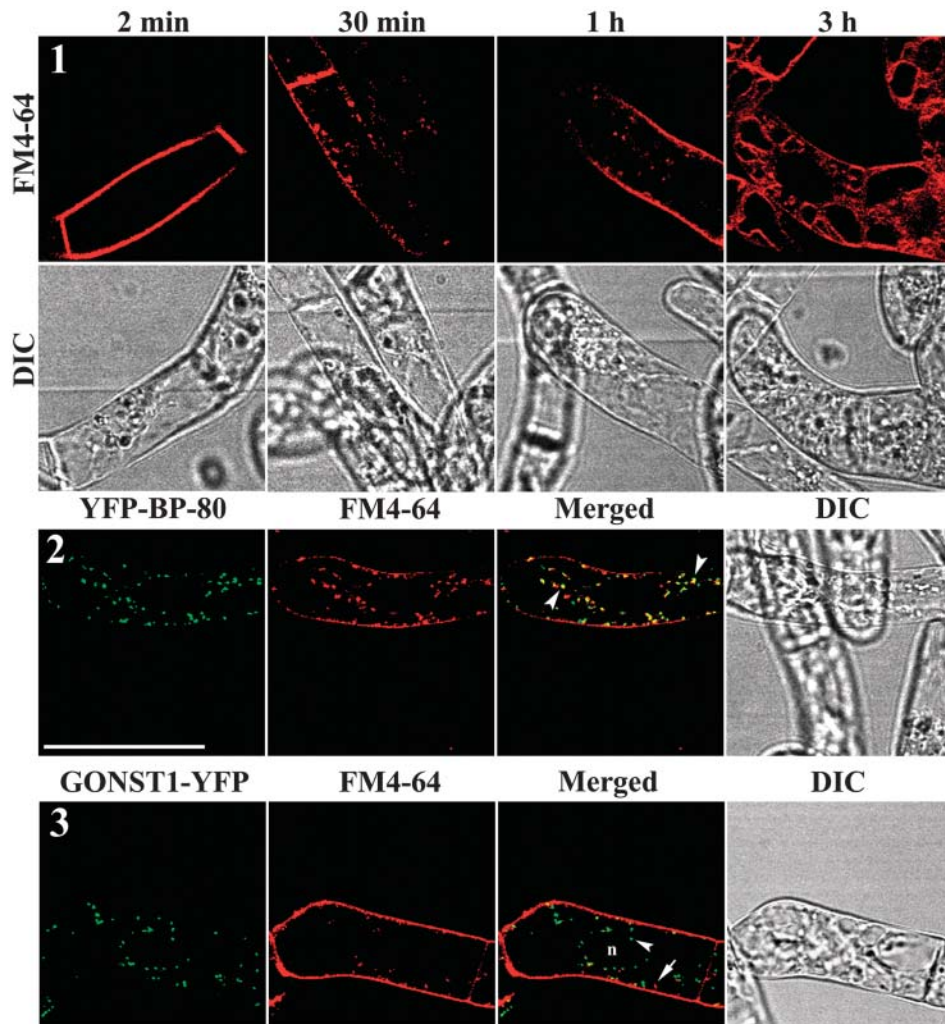


**Figure 14.** Colocalization of YFP-BP-80–Labeled PVCs with Internalized FM4-64–Marked Organelles in BY-2 Cells.

Panel 1, uptake process of FM4-64 in living cells. Shown are steps of FM4-64 uptake profiled in living BY-2 cells in which the dye is first detected on the plasma membrane, followed by localization in internalized endosome-like structures and eventually insertion in the tonoplast. Panels 2 and 3, colocalization of PVC reporters with internalized FM4-64–labeled organelles. At 30 min after uptake, FM4-64–marked organelles colocalized with YFP-labeled PVCs in cells expressing the YFP-BP-80 reporter (panel 2) but remained separate from YFP-labeled Golgi stacks in cells expressing the GONST1-YFP reporter (panel 3). Bar = 50  $\mu$ m.

(33  $\mu$ M) effectively inhibits plant PI-3K activity (Matsuoka et al., 1995) and also reduces the uptake of the styryl dye FM1-43 in BY-2 cells by  $\sim$ 40% (Emans et al., 2002). However, the intracellular target of wortmannin in plants had not previously been established. Our results clearly pinpoint the MVB/PVC as the site of action of wortmannin because treatment with this drug specifically effects the MVB/PVC, causing it to swell, to lose its surface plaque, and to have fewer internal vesicles.

### Concluding Remarks

In this article, we have been able to morphologically identify MVBs as being PVCs, thereby providing a function for these

frequently seen but hitherto puzzling structures. MVBs are enriched in VSRs, and this has enabled their successful isolation, which will now make them available for future proteome analysis (Mo et al., 2003). However, a whole new set of questions now arises, in particular because evidence that AtVSR<sub>1</sub> also functions as a receptor for storage proteins in seeds of Arabidopsis has been obtained (Shimada et al., 2004). It is now recognized that plant cells may contain functionally distinct vacuoles, so does this mean that there also are different PVCs? If so, are they morphologically distinct? The great majority of the vacuoles in BY-2 cells possess  $\gamma$ -TIP (Neuhaus, 2000) and are thus by definition lytic vacuoles. However, smaller PSVs may exist. If indeed AtVSR<sub>1</sub> plays a dual role in sorting both lytic and storage

proteins, probing with antibodies or (X)FP constructs of this protein may alone be insufficient for an adequate differentiation between PVC types.

## METHODS

General methods for construction of recombinant plasmids, characterization of cloned inserts, maintenance of *N. tabacum* culture cells, and preparation and characterization of antibodies have been described previously (Rogers et al., 1997; Jiang and Rogers, 1998; Cao et al., 2000; Jiang et al., 2000, 2001).

### Plasmid Construction

For the construction of pSYFP491K, the YFP sequence plus the signal peptide of proaleurain (Jiang and Rogers, 1998) were amplified by PCR from pGONST1-YFP (Baldwin et al., 2001) using the upstream primer YFP-F (5'-GGGGGATCCATGGCCACGCCGCGTCCTCCTCCTGGC-GCTCGCCGTCCTGGCCACGCCGCGCGTCGCGTCGCCAGTAAAGG-AGAAGAACCTTTTC-3') and the downstream primer YFP-R (3'-GGGGA-ATTCTTTGTATTGTCATCCATGCC-5'). The amplified PCR fragment then was digested with BamHI/EcoRI and subcloned into LJ491 construct (Jiang and Rogers, 1998) using the same restriction sites. The HindIII-35S promoter-SYFP-TMD-CT-SacI fragment then was subcloned into the binary vector pBI121. The resulting construct pSYFP491K thus contains the 35S promoter, followed by proaleurain signal peptide/YFP sequences, the spacer, and TMD/CT sequences of BP-80 (Jiang and Rogers, 1998). The construct was checked by both restriction mapping and sequencing.

### Transformation of BY-2 Cells

The above plasmid pSYFP491K was introduced into *A. tumefaciens* (strain LBA4404) by electroporation and used to transfect wild-type BY-2 cells. BY-2 cells are maintained in MS media by subculturing twice a week and culturing at room temperature in a shaker set at 125 rpm. Transfected BY-2 cells were transferred onto MS media (Sigma, St. Louis, MO) containing kanamycin (100 µg/mL) and cefotaxin (300 µg/mL) for 3 to 4 weeks until transformed colonies were formed. Resistant cell colonies (~50 to 100 from each construct) were subjected to screening for their expression and accumulation using confocal immunofluorescence. Selected cell lines (5 to 10 per construct) were further transferred into MS liquid media containing kanamycin to initiate suspension culture and used for subsequent analysis. Transgenic *N. tabacum* BY-2 cells were maintained in both liquid and solid culture via subculturing twice a week.

### Antibodies

A recombinant protein representing the luminal portion (lacking the TMD and CT) of VSR<sub>At-1</sub> (Paris et al., 1997) was expressed in *D. melanogaster* S2 cells (Cao et al., 2000; Li et al., 2002). Affinity-purified recombinant proteins then were used for immunization of two rabbits at the animal house of Chinese University of Hong Kong (CUHK). A synthetic peptide corresponding to the BP-80 CT sequences (Paris et al., 1997) was synthesized (Genemed Synthesis, San Francisco, CA) and conjugated to either BSA or KLH before immunization of two rabbits at CUHK. Antibodies were titred by serial dilution on dot blots of the recombinant protein or synthetic peptide versus preimmune serum. Antibodies were further purified by affinity chromatography using a column made with recombinant protein or synthetic peptide coupled to CnBr Sepharose (Sigma) as previously described (Rogers et al., 1997). The production of a polyclonal antibody specific for a Golgi-localized *Glycine max* (soybean)

α-1,2 anti-ManI was described previously (Li et al., 2002). Secondary Cy5-, lissamine rhodamine-, or fluorescein isothiocyanate-conjugated affinity-purified anti-rabbit or anti-mouse antibodies were purchased from Jackson ImmunoResearch Laboratories (West Grove, PA). GFP antibodies were purchased from Molecular Probes (Eugene, OR). For protein gel blot detection, ManI antibodies, GFP antibodies, and VSR antibodies were used at 10 µg/mL, whereas plasma membrane ATPase antibodies were used at 1:100 dilution.

### Confocal Immunofluorescence Studies

Fixation and preparation of *N. tabacum* BY2 cells and their labeling and analysis by epifluorescence and confocal immunofluorescence have been described previously (Jiang and Rogers, 1998; Jiang et al., 2000; Li et al., 2002). The settings for collecting confocal images within the linear range were as described (Jiang and Rogers, 1998). For immune double labeling, polyclonal rabbit and mouse monoclonal antibodies were incubated together or in order at 4°C overnight at the following working concentrations: 1:100 dilution for both anti-AtSYP21 and 4 µg/mL for anti-VSR and anti-GFP. All confocal fluorescence images were collected using a Bio-Rad Radiance 2100 system (Hemel Hempstead, UK). Images were processed using Adobe Photoshop software (San Jose, CA) as previously described (Jiang and Rogers, 1998).

The extent of colocalization of two antibodies or signal in confocal immunofluorescence images from BY2 cells was quantitated as described previously (Jiang and Rogers, 1998; Jiang et al., 2000). Controls to ascertain the specificity of double labeling experiments were performed as previously described (Jauh et al., 1999; Jiang et al., 2000). Briefly, for labeling using either two monoclonal or two polyclonal antibodies, primary antibodies were incubated at 4°C overnight (in PBS supplemented with 0.1% Triton X-100 [PBST] + 1% BSA) followed by washing in PBST. Rhodamine-conjugated Fab fragment then was added and incubated at room temperature for 4 h before a second wash, followed by addition of the second primary antibodies. For double labeling using one monoclonal and one polyclonal antibody, duplicate labeling of samples was performed, in which each primary antibody was added individually, followed by a wash and addition of the second primary antibody to ensure that either order of antibody application resulted in the same labeling results. Additionally, we confirmed that the labeling pattern for an antibody used individually matched the pattern obtained with the same antibody when used in double labeling experiments (Jiang et al., 2000; Li et al., 2002).

### FM4-64 Uptake Study

Two transgenic suspension BY-2 cell lines were used in the FM4-64 uptake study. Transgenic suspension cultured BY-2 cells first were washed with MS liquid media, and 0.5 µL of 12 µM FM4-64 was added to each 100 µL of culture and incubated at room temperature for 2 min. The FM4-64-treated cells then were washed with MS several times and mounted on a slide for time-course observation under a confocal microscope. All confocal fluorescence images were collected using a Bio-Rad Radiance 2100 system with a 60× objective oil lens, and the filter sets were used as follows: for YFP, excitation wavelength 514 nm, dichroic mirror 560DCLPXR, and emission filter HQ545/40; for FM4-64, excitation wavelength 543 nm and emission filter HQ660LP. Images were processed using Adobe Photoshop software as described previously (Jiang and Rogers, 1998).

### Isolation of PVCs

PVC isolation was performed at 4°C according to Shimada et al. (2002) with modification. BY-2 cells at the log phase (3 d after subculture) were

used for protoplast isolation. Packed BY-2 cells (15 mL) were incubated in the dark at 30°C in 20 mL of lysis buffer (1% cellulase, 0.05% pectinase, 0.5% driselase, and 0.4 M mannitol) for 2 h. The packed protoplasts (~5 mL) then were washed twice with 0.4 M mannitol and further lysed by four passages through a 25<sup>5/8</sup>-gauge needle and spun at 1000g for 10 min. The supernatant was collected and loaded on the top of a sucrose step gradient consisting of 5 mL of each of the following concentration 25, 40, 55, and 70% sucrose solution (w/v) in basic buffer (40 mM Hepes-NaOH, pH 7.2, 10 mM KCl, 3 mM MgCl<sub>2</sub>, and 0.1 mM EDTA). The gradient was subsequently centrifuged at 110,000g for 2 h. VSR-enriched PVC fractions were pooled and diluted three times with basic buffer and further applied on a 25 to 50% (w/w) linear sucrose gradient and centrifuged as described above. Each fraction (1 mL) of the gradient was collected and used for protein gel blot analysis as previously described (Li et al., 2002).

### Electron Microscopy of Resin-Embedded Cells

The general procedures for conventional thin sectioning of chemically fixed samples of BY-2 cells were performed essentially as described previously (Ritzenthaler et al., 2002). For high-pressure freezing suspension, cultured cells were harvested by filtering and immediately frozen in a high-pressure freezing apparatus (HPF010; Bal-Tec, Balzers, Liechtenstein). For subsequent freeze substitution, the material was kept at -85°C for 60 h before slowly being warmed to 0°C for a period of 18 h. Substitution was performed in an AFS freeze substitution unit (Leica, Bensheim, Germany). The substitution medium (dry acetone) was supplemented with 0.1% (w/v) uranyl acetate. After the sample reached 0°C, the medium was replaced with 100% ethanol, which was again changed to fresh 100% ethanol 10 min later. The cells then were stepwise infiltrated with London Resin White (hard grade) at room temperature, embedded, and heat polymerized as described previously (Ritzenthaler et al., 2002). Immunolabeling on London Resin White sections was done using standard procedures as described (Hohl et al., 1996), with VSR antibodies at a primary dilution of 1:100 and gold-coupled secondary antibodies at 1:30. Aqueous uranyl acetate/lead citrate poststained sections were examined in a Philips CM10 transmission electron microscope (Eindhoven, The Netherlands) operating at 80 kV.

### ImmunoEM Detection of Isolated PVC

The fractions containing pure PVCs as identified by VSR antibodies were diluted five times with water. Five-milliliter sample aliquots were air dried onto a carbon-coated 400-mesh gold grid and negatively stained for immediate electron microscopy observation. For immunoEM labeling, the grid with the specimen was floated upside down on 30 mL of aliquots of VSR antibody (40 µg/mL diluted with PBS containing 1% BSA-PBS-BSA) for 30 min, followed by washing by floating on four droplets of PBS-BSA for 1 min each. The grid then was floated on 30 mL of aliquots of gold-conjugated secondary antibody (30 times diluted with PBS-BSA) for 30 min and rinsed by floating grid three times for 1 min each on droplets of water. Grids were finally stained with 5% uranyl acetate before electron microscopy observation.

### ACKNOWLEDGMENTS

We are grateful to J.C. Rogers (Washington State University, Pullman, WA) for VSR<sub>At-1</sub> recombinant protein and M. Maeshima (Nagoya University, Japan) for sharing various antibodies, including anti-ATPase. We thank P. Dupree (University of Cambridge, UK) for the pGONST1-YFP construct. We also thank N.V. Raikhel (University of California, Riverside, CA) for sharing anti-AtSYP21p antibodies. This work is

supported by grants from CUHK, Research Grants Council of Hong Kong (CUHK4156/01M, CUHK4260/02M, and CUHK4307/03M), from Hong Kong/German, Hong Kong/France Research Scheme, and University Grants Council for Area of Excellence to L.J., and from the Human Frontiers in Science Program and German Academic Exchange Service to D.G.R. B.M. is partially supported by a postdoctoral fellowship from CUHK. A portion of this work has been presented in abstract form for a poster for the American Society of Plant Biologists Annual Meeting 2003 (<http://abstracts.aspb.org/pb2003/public/P68/0775.html>).

Received December 2, 2003; accepted December 20, 2003.

### REFERENCES

- Ahmed, S.U., Bar-Peled, M., and Raikhel, N.V. (1997). Cloning and subcellular location of an Arabidopsis receptor-like protein that shares common features with protein-sorting receptors of eukaryotic cells. *Plant Physiol.* **114**, 325–336.
- Ahmed, S.U., Rojo, E., Kovaleva, V., Venkataraman, S., Dombrowski, J.E., Matsuoka, K., and Raikhel, N.V. (2000). The plant vacuolar sorting receptor AtELP is involved in transport of NH<sub>2</sub>-terminal propeptide-containing vacuolar proteins in Arabidopsis thaliana. *J. Cell Biol.* **149**, 1335–1344.
- Aniento, F., Helms, J.B., and Memon, A.R. (2003). How to make a vesicle: Coat protein-membrane interactions. *Annu. Plant Rev.* **9**, 36–62.
- Baldwin, T.C., Handford, M.G., Yuseff, M.I., Orellana, A., and Dupree, P. (2001). Identification and characterization of GONST1, a golgi-localized GDP-mannose transporter in Arabidopsis. *Plant Cell* **13**, 2283–2295.
- Barr, F.A. (2002). Inheritance of the endoplasmic reticulum and Golgi apparatus. *Curr. Opin. Cell Biol.* **14**, 496–499.
- Bassham, D.C., Gal, S., da Silva, C.A., and Raikhel, N.V. (1995). An Arabidopsis syntaxin homologue isolated by functional complementation of a yeast pep12 mutant. *Proc. Natl. Acad. Sci. USA* **92**, 7262–7266.
- Batley, N.H., James, N.C., Greenland, A.J., and Brownlee, C. (1999). Exocytosis and endocytosis. *Plant Cell* **11**, 643–660.
- Boehm, M., and Bonifacino, J.S. (2001). Adaptins: The final recount. *Mol. Biol. Cell* **12**, 2907–2920.
- Bolte, S., Brown, S., and Satiat-Jeunemaitre, B. (2004). The N-myristoylated Rab-GTPase mRabmc is involved in post-Golgi trafficking events to the lytic vacuole in plant cells. *J. Cell Sci.*, in press.
- Bright, N.A., Lindsay, M.R., Stewart, A., and Luzio, J.P. (2001). The relationship between luminal and limiting membranes in swollen late endocytic compartments formed after wortmannin treatment or sucrose accumulation. *Traffic* **2**, 631–642.
- Cao, X., Rogers, S.W., Butler, J., Beevers, L., and Rogers, J.C. (2000). Structural requirements for ligand binding by a probable plant vacuolar sorting receptor. *Plant Cell* **12**, 493–506.
- Conceição, A.S., Marty-Mazars, D., Bassham, D.C., Sanderfoot, A.A., Marty, F., and Raikhel, N.V. (1997). The syntaxin homolog AtPEP12p resides on a late post-Golgi compartment in plants. *Plant Cell* **9**, 571–582.
- Conibear, E., and Stevens, T.H. (1998). Multiple sorting pathways between the late Golgi and the vacuole in yeast. *Biochim. Biophys. Acta* **1404**, 211–230.
- Cooper, A.A., and Stevens, T.H. (1996). Vps10p cycles between the late-Golgi and prevacuolar compartments in its function as the

- sorting receptor for multiple yeast vacuolar hydrolases. *J. Cell Biol.* **133**, 529–541.
- Corvera, S., D'Arrigo, A., and Stenmark, H.** (1999). Phosphoinositides in membrane traffic. *Curr. Opin. Cell Biol.* **11**, 460–465.
- Culianez-Macia, F.A., and Martin, C.** (1993). DIP: A member of the MIP family of membrane proteins that is expressed in mature seeds and dark-grown seedlings of *Antirrhinum majus*. *Plant J.* **4**, 717–725.
- Di Sanebastiano, G.P., Paris, N., Marc-Martin, S., and Neuhaus, J.M.** (1998). Specific accumulation of GFP in a non-acidic vacuolar compartment via a C-terminal propeptide-mediated sorting pathway. *Plant J.* **15**, 449–457.
- Emans, N., Zimmermann, S., and Fischer, R.** (2002). Uptake of a fluorescent marker in plant cells is sensitive to brefeldin A and wortmannin. *Plant Cell* **14**, 71–86.
- Fernandez-Borja, M., Wubbolts, R., Calafat, J., Janssen, H., Divecha, N., Dusseljee, S., and Neefjes, J.** (1999). Multivesicular body morphogenesis requires phosphatidylinositol 3-kinase activity. *Curr. Biol.* **9**, 55–58.
- Frigerio, L., de Virgilio, M., Prada, A., Faoro, F., and Vitale, A.** (1998). Sorting of phaseolin to the vacuole is saturable and requires a short C-terminal peptide. *Plant Cell* **10**, 1031–1042.
- Futter, C.E., Pearse, A., Hewlett, L.J., and Hopkins, C.R.** (1996). Multivesicular endosomes containing internalized EGF-EGF receptor complexes mature and then fuse directly with lysosomes. *J. Cell Biol.* **132**, 1011–1023.
- Galway, M.E., Rennie, P.J., and Fowke, L.C.** (1993). Ultrastructure of the endocytotic pathway in glutaraldehyde-fixed and high-pressure frozen/freez-substituted protoplasts of white spruce (*Picea glauca*). *J. Cell Sci.* **106**, 847–858.
- Gaullier, J.M., Simonsen, A., D'Arrigo, A., Bremnes, B., Stenmark, H., and Aasland, R.** (1998). FYVE fingers bind PtdIns(3)P. *Nature* **394**, 432–433.
- Gerrard, S.R., Bryant, N.J., and Stevens, T.H.** (2000a). VPS21 controls entry of endocytosed and biosynthetic proteins into the yeast prevacuolar compartment. *Mol. Biol. Cell* **11**, 613–626.
- Gerrard, S.R., Levi, B.P., and Stevens, T.H.** (2000b). Pep12p is a multifunctional yeast syntaxin that controls entry of biosynthetic, endocytic and retrograde traffic into the prevacuolar compartment. *Traffic* **1**, 259–269.
- Ghosh, P., Dahms, N.M., and Kornfeld, S.** (2003). Mannose 6-phosphate receptors: New twists in the tale. *Nat. Rev. Mol. Cell Biol.* **4**, 2002–2012.
- Gillooly, D.J., Morrow, I.C., Lindsay, M., Gould, R., Bryant, N.J., Gaullier, J.M., Parton, R.G., and Stenmark, H.** (2000). Localization of phosphatidylinositol 3-phosphate in yeast and mammalian cells. *EMBO J.* **19**, 4577–4588.
- Graham, T.R., and Nothwehr, S.F.** (2002). Protein transport to the yeast vacuole. In *Protein Targeting, Transport and Translocation*, R.E. Dalbey and G. von Heijne, eds (Amsterdam: Academic Press), pp. 322–357.
- Griffiths, G., Hoflack, B., Simons, K., Mellman, I., and Kornfeld, S.** (1988). The mannose 6-phosphate receptor and the biogenesis of lysosomes. *Cell* **52**, 329–341.
- Griffiths, G., Matteoni, R., Back, R., and Hoflack, B.** (1990). Characterization of the cation-independent mannose 6-phosphate receptor-enriched prelysosomal compartment in NRK cells. *J. Cell Sci.* **95**, 441–461.
- Gu, F., and Gruenberg, J.** (1999). Biogenesis of transport intermediates in the endocytic pathway. *FEBS Lett.* **452**, 61–66.
- Hadlington, J.L., and Denecke, J.** (2000). Sorting of soluble proteins in the secretory pathway of plants. *Curr. Opin. Plant Biol.* **3**, 461–468.
- Hara-Nishimura, I.I., Shimada, T., Hatano, K., Takeuchi, Y., and Nishimura, M.** (1998). Transport of storage proteins to protein storage vacuoles is mediated by large precursor-accumulating vesicles. *Plant Cell* **10**, 825–836.
- Hille-Rehfeldt, A.** (1995). Mannose 6-phosphate receptors in sorting and transport of lysosomal enzymes. *Biochim. Biophys. Acta* **1241**, 177–194.
- Hillmer, S., Depta, H., and Robinson, D.G.** (1986). Confirmation of endocytosis in higher plant protoplasts using lectin-gold conjugates. *Eur. J. Cell Biol.* **42**, 142–149.
- Hillmer, S., Movafeghi, A., Robinson, D.G., and Hinz, G.** (2001). Vacuolar storage proteins are sorted in the cis-cisternae of the pea cotyledon Golgi apparatus. *J. Cell Biol.* **152**, 41–50.
- Hinz, G., and Herman, E.M.** (2003). Sorting of storage proteins in the plant Golgi apparatus. *Annu. Plant Rev.* **9**, 141–164.
- Hinz, G., Hillmer, S., Baumer, M., and Hohl, I.** (1999). Vacuolar storage proteins and the putative vacuolar sorting receptor BP-80 exit the golgi apparatus of developing pea cotyledons in different transport vesicles. *Plant Cell* **11**, 1509–1524.
- Hirst, J., Futter, C.E., and Hopkins, C.R.** (1998). The kinetics of mannose 6-phosphate receptor trafficking in the endocytic pathway in HEp-2 cells: The receptor enters and rapidly leaves multivesicular endosomes without accumulating in a prelysosomal compartment. *Mol. Biol. Cell* **9**, 809–816.
- Hohl, I., Robinson, D.G., Chrispeels, M.J., and Hinz, G.** (1996). Transport of storage proteins to the vacuole is mediated by vesicles without a clathrin coat. *J. Cell Sci.* **109**, 2539–2550.
- Holstein, S.E.** (2002). Clathrin and plant endocytosis. *Traffic* **3**, 614–620.
- Humair, D., Hernandez, F.D., Neuhaus, J.M., and Paris, N.** (2001). Demonstration in yeast of the function of BP-80, a putative plant vacuolar sorting receptor. *Plant Cell* **13**, 781–792.
- Jackson, C.L., and Casanova, J.E.** (2000). Turning on ARF: The Sec7 family of guanine-nucleotide-exchange factors. *Trends Cell Biol.* **10**, 60–67.
- Jauh, G.Y., Phillips, T.E., and Rogers, J.C.** (1999). Tonoplast intrinsic protein isoforms as markers for vacuolar functions. *Plant Cell* **11**, 1867–1882.
- Jiang, L., Erickson, A., and Rogers, J.** (2002). Multivesicular bodies: A mechanism to package lytic and storage functions in one organelle? *Trends Cell Biol.* **12**, 362–367.
- Jiang, L., Phillips, T.E., Hamm, C.A., Drozdowicz, Y.M., Rea, P.A., Maeshima, M., Rogers, S.W., and Rogers, J.C.** (2001). The protein storage vacuole: A unique compound organelle. *J. Cell Biol.* **155**, 991–1002.
- Jiang, L., Phillips, T.E., Rogers, S.W., and Rogers, J.C.** (2000). Biogenesis of the protein storage vacuole crystalloid. *J. Cell Biol.* **150**, 755–770.
- Jiang, L., and Rogers, J.C.** (1998). Integral membrane protein sorting to vacuoles in plant cells: Evidence for two pathways. *J. Cell Biol.* **143**, 1183–1199.
- Jiang, L., and Rogers, J.C.** (2003). Sorting of lytic enzymes in the plant Golgi apparatus. *Annu. Plant Rev.* **9**, 114–140.
- Kil, S.J., Hobert, M., and Carlin, C.** (1999). A leucine-based determinant in the epidermal growth factor receptor juxtamembrane domain is required for the efficient transport of ligand-receptor complexes to lysosomes. *J. Biol. Chem.* **274**, 3141–3150.
- Kim, D.H., Eu, Y.J., Yoo, C.M., Kim, Y.W., Pih, K.T., Jin, J.B., Kim, S.J., Stenmark, H., and Hwang, I.** (2001). Trafficking of Phosphatidylinositol 3-Phosphate from the trans-Golgi Network to the Lumen of the Central Vacuole in Plant Cells. *Plant Cell* **13**, 287–301.
- Kirsch, T., Saalbach, G., Raikhel, N.V., and Beevers, L.** (1996). Interaction of a potential vacuolar targeting receptor with amino- and carboxyl-terminal targeting determinants. *Plant Physiol.* **111**, 469–474.



- Klausner, R.D., Donaldson, J.G., and Lippincott-Schwartz, J.** (1992). Brefeldin A: Insights into the control of membrane traffic and organelle structure. *J. Cell Biol.* **116**, 1071–1080.
- Klumperman, J., Hille, A., Veenendaal, T., Oorschot, V., Stoorvogel, W., von Figura, K., and Geuze, H.J.** (1993). Differences in the endosomal distributions of the two mannose 6-phosphate receptors. *J. Cell Biol.* **121**, 997–1010.
- Kobayashi, T., Stang, E., Fang, K.S., de Moerloose, P., Parton, R.G., and Gruenberg, J.** (1998). A lipid associated with the antiphospholipid syndrome regulates endosome structure and function. *Nature* **392**, 193–197.
- Koide, Y., Hirano, H., Matsuoka, K., and Nakamura, K.** (1997). The N-terminal propeptide of the precursor to sporamin acts as a vacuole-targeting signal even at the C terminus of the mature part in tobacco cells. *Plant Physiol.* **114**, 863–870.
- Le Borgne, R., and Hoflack, B.** (1998). Protein transport from the secretory to the endocytic pathway in mammalian cells. *Biochim. Biophys. Acta* **1404**, 195–209.
- Lemmon, S.K., and Traub, L.M.** (2000). Sorting in the endosomal system in yeast and animal cells. *Curr. Opin. Cell Biol.* **12**, 457–466.
- Li, Y.B., Rogers, S.W., Tse, Y.C., Lo, S.W., Sun, S.S., Jauh, G.Y., and Jiang, L.** (2002). BP-80 and homologs are concentrated on post-Golgi, probable lytic prevacuolar compartments. *Plant Cell Physiol.* **43**, 726–742.
- Luzio, J.P., Poupon, V., Lindsay, M.R., Mullock, B.M., Piper, R.C., and Pryor, P.R.** (2003). Membrane dynamics and the biogenesis of lysosomes. *Mol. Membr. Biol.* **20**, 141–154.
- Luzio, J.P., Rous, B.A., Bright, N.A., Pryor, P.R., Mullock, B.M., and Piper, R.C.** (2000). Lysosome-endosome fusion and lysosome biogenesis. *J. Cell Sci.* **113**, 1515–1524.
- Matsuoka, K., Bassham, D.C., Raikhel, N.V., and Nakamura, K.** (1995). Different sensitivity to wortmannin of two vacuolar sorting signals indicates the presence of distinct sorting machineries in tobacco cells. *J. Cell Biol.* **130**, 1307–1318.
- Mo, B., Tse, Y.C., and Jiang, L.** (2003). Organelle identification and proteomics in plant cells. *Trends Biotechnol.* **21**, 331–332.
- Mulholland, J., Konopka, J., Singer-Kruger, B., Zerial, M., and Botstein, D.** (1999). Visualization of receptor-mediated endocytosis in yeast. *Mol. Biol. Cell* **10**, 799–817.
- Nakamura, K., Matsuoka, K., Mukumoto, F., and Watanabe, N.** (1993). Processing and transport to the vacuole of a precursor to sweet potato sporamin in transformed tobacco cell line BY-2. *J. Exp. Bot.* **44** (suppl.), 331–338.
- Nebenführ, A., Gallagher, L.A., Dunahay, T.G., Frohlick, J.A., Mazurkiewicz, A.M., Meehl, J.B., and Staehelin, L.A.** (1999). Stop-and-go movements of plant Golgi stacks are mediated by the actomyosin system. *Plant Physiol.* **121**, 1127–1142.
- Nebenführ, A., Ritzenthaler, C., and Robinson, D.G.** (2002). Brefeldin A: Deciphering an enigmatic inhibitor of secretion. *Plant Physiol.* **130**, 1102–1108.
- Neuhaus, J.-M.** (2000). GFP as a marker for vacuoles in plants. *Annu. Plant Rev.* **5**, 254–269.
- Neuhaus, J.M., and Rogers, J.C.** (1998). Sorting of proteins to vacuoles in plant cells. *Plant Mol. Biol.* **38**, 127–144.
- Okita, T.W., and Rogers, J.C.** (1996). Compartmentation of proteins in the endomembrane system of plant cells. *Annu. Rev. Plant Physiol. Plant Mol. Biol.* **47**, 327–350.
- Paris, N., and Neuhaus, J.M.** (2002). BP-80 as a vacuolar sorting receptor. *Plant Mol. Biol.* **50**, 903–914.
- Paris, N., Rogers, S.W., Jiang, L., Kirsch, T., Beevers, L., Phillips, T.E., and Rogers, J.C.** (1997). Molecular cloning and further characterization of a probable plant vacuolar sorting receptor. *Plant Physiol.* **115**, 29–39.
- Parton, R.G., Schrotz, P., Bucci, C., and Gruenberg, J.** (1992). Plasticity of early endosomes. *J. Cell Sci.* **103**, 335–348.
- Puertollano, R., Aguilar, R.C., Gorshkova, I., Crouch, R.J., and Bonifacino, J.S.** (2001). Sorting of mannose 6-phosphate receptors mediated by the GGAs. *Science* **292**, 1712–1716.
- Raposo, G., Tenza, D., Murphy, D.M., Berson, J.F., and Marks, M.S.** (2001). Distinct protein sorting and localization to premelanosomes, melanosomes, and lysosomes in pigmented melanocytic cells. *J. Cell Biol.* **152**, 809–824.
- Reaves, B.J., Bright, N.A., Mullock, B.M., and Luzio, J.P.** (1996). The effect of wortmannin on the localisation of lysosomal type I integral membrane glycoproteins suggests a role for phosphoinositide 3-kinase activity in regulating membrane traffic late in the endocytic pathway. *J. Cell Sci.* **109**, 749–762.
- Record, R.D., and Griffing, L.R.** (1988). Convergence of the endocytic and lysosomal pathways in soybean protoplasts. *Planta* **176**, 425–432.
- Reggiori, F., Black, M.W., and Pelham, H.R.** (2000). Polar transmembrane domains target proteins to the interior of the yeast vacuole. *Mol. Biol. Cell* **11**, 3737–3749.
- Reggiori, F., and Pelham, H.R.** (2001). Sorting of proteins into multivesicular bodies: Ubiquitin-dependent and -independent targeting. *EMBO J.* **20**, 5176–5186.
- Ritzenthaler, C., Nebenführ, A., Movafeghi, A., Stussi-Garaud, C., Behnia, L., Pimpl, P., Staehelin, L.A., and Robinson, D.G.** (2002). Reevaluation of the effects of brefeldin A on plant cells using tobacco Bright Yellow 2 cells expressing Golgi-targeted green fluorescent protein and COPI antisera. *Plant Cell* **14**, 237–261.
- Robinson, D.G., and Hinz, G.** (1999). Golgi-mediated transport of seed storage proteins. *Seed Sci. Res.* **9**, 267–283.
- Robinson, D.G., Hinz, G., and Holstein, S.E.** (1998). The molecular characterization of transport vesicles. *Plant Mol. Biol.* **38**, 49–76.
- Robinson, D.G., and Ritzenthaler, C.** (2003). Perturbation of ER-Golgi vesicle trafficking. *Annu. Plant Rev.* **9**, 193–207.
- Robinson, D.G., Rogers, J.C., and Hinz, G.** (2000). Post-Golgi, prevacuolar compartments. *Annu. Plant Rev.* **5**, 270–298.
- Rodman, J.S., and Wandlinger-Ness, A.** (2000). Rab GTPases coordinate endocytosis. *J. Cell Sci.* **113**, 183–192.
- Rogers, S.W., Burks, M., and Rogers, J.C.** (1997). Monoclonal antibodies to barley aleurain and homologs from other plants. *Plant J.* **11**, 1359–1368.
- Saalbach, G., Jung, R., Kunze, G., Saalbach, I., Adler, K., and Müntz, K.** (1991). Different legumin protein domains act as vacuolar targeting signals. *Plant Cell* **3**, 695–708.
- Sachse, M., Urbe, S., Oorschot, V., Strous, G.J., and Klumperman, J.** (2002). Bilayered clathrin coats on endosomal vacuoles are involved in protein sorting toward lysosomes. *Mol. Biol. Cell* **13**, 1313–1328.
- Sanderfoot, A.A., Ahmed, S.U., Marty-Mazars, D., Rapoport, I., Kirchhausen, T., Marty, F., and Raikhel, N.V.** (1998). A putative vacuolar cargo receptor partially colocalizes with AtPEP12p on a prevacuolar compartment in Arabidopsis roots. *Proc. Natl. Acad. Sci. USA* **95**, 9920–9925.
- Satiat-Jeunemaitre, B., and Hawes, C.** (1992). Redistribution of a Golgi glycoprotein in plant cells treated with Brefeldin A. *J. Cell Sci.* **103**, 1153–1166.
- Scales, S.J., Gomez, M., and Kreis, T.E.** (2000). Coat proteins regulating membrane traffic. *Int. Rev. Cytol.* **195**, 67–144.
- Schu, P.V., Takegawa, K., Fry, M.J., Stack, J.H., Waterfield, M.D., and Emr, S.D.** (1993). Phosphatidylinositol 3-kinase encoded by yeast VPS34 gene essential for protein sorting. *Science* **260**, 88–91.
- Sciaky, N., Presley, J., Smith, C., Zaal, K.J., Cole, N., Moreira, J.E., Terasaki, M., Siggia, E., and Lippincott-Schwartz, J.** (1997). Golgi

- tubule traffic and the effects of brefeldin A visualized in living cells. *J. Cell Biol.* **139**, 1137–1155.
- Shimada, T., Fuji, K., Tamura, K., Nishimura, M., and Hara-Nishimura, I.** (2004). Vacuolar sorting receptor for seed storage proteins in *Arabidopsis thaliana*. *Proc. Natl. Acad. Sci. USA*, in press.
- Shimada, T., Kuroyanagi, M., Nishimura, M., and Hara-Nishimura, I.** (1997). A pumpkin 72-kDa membrane protein of precursor-accumulating vesicles has characteristics of a vacuolar sorting receptor. *Plant Cell Physiol.* **38**, 1414–1420.
- Shimada, T., Watanabe, E., Tamura, K., Hayashi, Y., Nishimura, M., and Hara-Nishimura, I.** (2002). A vacuolar sorting receptor PV72 on the membrane of vesicles that accumulate precursors of seed storage proteins (PAC vesicles). *Plant Cell Physiol.* **43**, 1086–1095.
- Sohn, E.J., Kim, E.S., Zhao, M., Kim, S.J., Kim, H., Kim, Y.W., Lee, Y.J., Hillmer, S., Sohn, U., Jiang, L., and Hwang, I.** (2003). Rha1, an *Arabidopsis* Rab5 homolog, plays a critical role in the vacuolar trafficking of soluble cargo proteins. *Plant Cell* **15**, 1057–1070.
- Tall, G.G., Hama, H., DeWald, D.B., and Horazdovsky, B.F.** (1999). The phosphatidylinositol 3-phosphate binding protein Vac1p interacts with a Rab GTPase and a Sec1p homologue to facilitate vesicle-mediated vacuolar protein sorting. *Mol. Biol. Cell* **10**, 1873–1889.
- Ueda, T., Yamaguchi, M., Uchimiya, H., and Nakano, A.** (2001). Ara6, a plant-unique novel type Rab GTPase, functions in the endocytic pathway of *Arabidopsis thaliana*. *EMBO J.* **20**, 4730–4741.
- van Dam, E.M., and Stoorvogel, W.** (2002). Dynamin-dependent transferrin receptor recycling by endosome-derived clathrin-coated vesicles. *Mol. Biol. Cell* **13**, 169–182.
- van Deurs, B., Holm, P.K., Kayser, L., Sandvig, K., and Hansen, S.H.** (1993). Multivesicular bodies in HEp-2 cells are maturing endosomes. *Eur. J. Cell Biol.* **61**, 208–224.
- Vanhaesebroeck, B., Leever, S.J., Panayotou, G., and Waterfield, M.D.** (1997). Phosphoinositide 3-kinases: A conserved family of signal transducers. *Trends Biochem. Sci.* **22**, 267–272.
- Vida, T.A., and Emr, S.D.** (1995). A new vital stain for visualizing vacuolar membrane dynamics and endocytosis in yeast. *J. Cell Biol.* **128**, 779–792.
- Vieira, O.V., Bucci, C., Harrison, R.E., Trimble, W.S., Lanzetti, L., Gruenberg, J., Schreiber, A.D., Stahl, P.D., and Grinstein, S.** (2003). Modulation of Rab5 and Rab7 recruitment to phagosomes by phosphatidylinositol 3-kinase. *Mol. Cell. Biol.* **23**, 2501–2514.
- Wee, E.G., Sherrier, D.J., Prime, T.A., and Dupree, P.** (1998). Targeting of active sialyltransferase to the plant Golgi apparatus. *Plant Cell* **10**, 1759–1768.
- Wurmser, A.E., and Emr, S.D.** (1998). Phosphoinositide signaling and turnover: PtdIns(3)P, a regulator of membrane traffic, is transported to the vacuole and degraded by a process that requires luminal vacuolar hydrolase activities. *EMBO J.* **17**, 4930–4942.
- Zerial, M., and McBride, H.** (2001). Rab proteins as membrane organizers. *Nat. Rev. Mol. Cell Biol.* **2**, 107–117.